# Parallel but distinct adaptive routes in the budding and fission yeasts after 10,000 generations of experimental evolution

**Authors**: Arnaud N'Guessan[1], Vivian Wang[1], Joao Ascensao[2], Christopher W. Bakerlee[2,3,4], Jenya Belousova[2], Greta Brenna[2], Megan E. Dillingham[5], Thomas Dupic[2], Shreyas Gopalakrishnan[2], Juhee Goyal[2,6], Misha Gupta[2], Caroline Holmes[2], Parris T. Humphrey[2,4], Tanush Jagdish[2,4,5], Elizabeth R. Jerison[2,7,8], Milo S. Johnson[2,4], Katya Kosheleva[2,8], Katherine R. Lawrence[2,4,9], Jiseon Min[2,3,4,6], Alief Moulana[2], Shreyas V. Pai[2,5], Angela M. Phillips[2], Julia C. Piper[8,10], Alexandra Poret[2,8,11], Ramya Purkanti[2,12], Artur Rego-Costa[2], Tatiana Ruiz-Bedoya[2], Cecilia Trivellin[2], Michael J. McDonald[2,13], Michael M. Desai[2,4,8], Alex N. Nguyen Ba[1,14]

1. Department of Cell and Systems Biology, University of Toronto, Ramsay Wright Laboratories, 25 Harbord St, M5S 3G5, Toronto, Ontario, Canada.
2. Department of Organismic and Evolutionary Biology, Harvard University, Cambridge MA 02138, USA
3. Department of Molecular and Cellular Biology, Harvard University, Cambridge, United States.
4. NSF-Simons Center for Mathematical and Statistical Analysis of Biology, Harvard University, Cambridge, United States.
5. Graduate Program in Systems, Synthetic, and Quantitative Biology, Harvard University, Cambridge, United States
6. John A Paulson School of Engineering and Applied Sciences, Harvard University, Cambridge, United States.
7. Department of Applied Physics, Stanford University, Stanford, United States.
8. Department of Physics, Harvard University, Cambridge MA 02138, USA
9. Department of Physics, Massachusetts Institute of Technology, Cambridge, United States.
10. AeroLabs, Aeronaut Brewing Co, Somerville, United States.
11. Graduate Program in Biophysics, Harvard University, Cambridge, MA, USA
12. The Max Planck Institute of Molecular Cell Biology and Genetics, Dresden, Germany.
13. School of Biological Sciences, Monash University, Clayton, Victoria, Australia
14. Department of Biology, University of Toronto at Mississauga, 3359 Mississauga Rd, L5L 1C6, Mississauga, Ontario, Canada

## ABSTRACT

Quantitative genetics approaches designed to understand the evolution of traits have helped improve our understanding of the genetic basis of adaptation. However, they often overlook crucial aspects of adaptation, including the long-term temporal evolutionary dynamics, the predictability of evolutionary outcomes, the influence of past evolution on future evolutionary trajectories (contingency), and the diversity of molecular mechanisms underlying adaptation. Experimental evolution has been a useful tool for answering these questions, but extracting fundamental principles and predictive features of evolutionary outcomes from these datasets remains challenging due to the large number of covariates and confounding effects, such as differences in experimental setup, species lifestyle, gene content, and evolution rate. Here, we

sought to circumvent these challenges by comparing distant yeast species that share several evolutionary features but differ mainly in evolutionary history and genome architecture, i.e. *Saccharomyces cerevisiae* and *Schizosaccharomyces pombe*. Thus, we evolved 10 populations of the fission yeast for 10,000 generations in the same conditions as a pre-existing budding yeast dataset (i.e. high-sugar media and hypoxic conditions), allowing us to observe repeatable evolutionary outcomes within species but diverse molecular mechanisms and targets of adaptation across species. The most frequent adapting route in these conditions involved upregulating fermentation genes and downregulating the glycolysis gene *pyk1*, which has not previously been observed in *S. cerevisiae* evolved populations or in wild *Kluyveromyces lactis,* but similar evolutionary paths have been observed in *Schizosaccharomyces japonicus* and in clinically relevant populations, such as some cancer cells. This suggests that parallelism is pervasive in the tree of life and that mechanisms of adaptation can be shared among closely related or distant species. Despite similar gene content and identical environments, recurrent adaptation across *S. pombe* populations involved different genes than in *S. cerevisiae* and was mostly detectable at the transcriptomic level. This suggests that trans-regulatory effects may play an important role in adaptation on short evolutionary timescales and that differences in evolutionary outcomes between these species may be attributed to contingency.

## INTRODUCTION

Long-term experimental evolution has highlighted the predictability of high-level features of evolution like fitness trajectories[1–6]. While fitness gains follow a fairly reproducible pattern of declining adaptability, the exact mutations or the sequence in which they occur are typically unpredictable. Nevertheless, experimental evolution done in large replication with the budding yeast *Saccharomyces cerevisiae* has revealed extensive parallelism at the gene or pathway level[3,7,8], even across strains that differed by thousands of polymorphisms[9]. These general patterns of reproducibility during experimental evolution are also seen in different organisms. For instance, during the *Escherichia coli* Long-Term Experimental Evolution (LTEE), half of the populations evolved a mutator phenotype and quasi-stable lineage coexistence emerged in 75% of the populations[4]. Further, substantial parallelism at the gene level can also be observed throughout the 12 populations over (now greater than) 60,000 generations[4].

Unsurprisingly, the molecular targets of selection during these experiments differ substantially between *S. cerevisiae* and *E. coli*[3,6]. Likewise, comparing microbial laboratory evolution to experimental evolution done in *Caenorhabditis elegans* and *Drosophila melanogaster* does not reveal universal targets of adaptation[10,11]. Notwithstanding their vastly different gene content and cellular form, part of the reason for these differences in molecular adaptation is the different selection environments between experiments (the LTEE was done in DM25 minimal media, while yeast was done in YPD rich media or in synthetic dextrose complete media). However, another more interesting hypothesis for these differences relates to the role of evolutionary contingency in shaping the dynamics and targets of selection.

Contingency is the product of past evolution, whereby epistasis and genome structures can strongly influence future adaptive potential[1,12,13]. Thus, species can be constrained to alternative adaptive paths, leading to profoundly different molecular signatures of evolution. Contingency has been explored in the context of strains with different gene deletions[13–16] and has even been observed in experimental evolution. For instance, across the 12 *E. coli* populations evolving in the same conditions during the LTEE, one population developed the ability to grow aerobically on citrate, a rare phenotype in this species resulting from a rare genome rearrangement. This phenotype is far more readily evolvable within that population after this rearrangement[17]. Further, while half of the LTEE populations evolved a mutator phenotype, and 75% evolved stable lineage coexistence, these phenomena are not observed in *S. cerevisiae* laboratory evolution experiments in standard rich media or in minimal media, despite being entirely capable of achieving these through genetic engineering[18].

While studying evolution using very distinct organisms has provided important insights into general features of evolutionary dynamics, it has made it difficult to discern the effect of life history from other idiosyncrasies on the molecular targets of selection. Would we find the same targets of selection (genes), and a preference for the same molecular mechanisms if we had evolved a species with substantially similar gene contents to that of *E. coli* or *S. cerevisiae*? The difficulty in answering this question is also reinforced by the wide variety of mechanisms of rapid adaptation revealed by long-term evolution studies, e.g. hybridization, selection on standing variation, cross-feeding interactions, or phenotypic plasticity involving behavioral or transcriptomic changes[11].

Evaluating the impact of differences between such species on quantitative trait evolution could improve our understanding of the role of genetic architecture and life history in trait diversity.

One way to address how much these two factors might influence short- and long-term adaptation is through the yeast subphylum. Although it exhibits immense trait diversity and is as genetically diverse as the animal kingdom[19,20], species within have a comparable number of genes, and share many genes and metabolic pathways such that most species can grow in the same media. As an example, *Saccharomyces cerevisiae* and *Schizosaccharomyces pombe* share about 4,500 genes (out of approximately 6,000), but are so diverged that their genomes show no synteny[21,22]. Evolutionarily, they have similar spontaneous mutation rates and were both domesticated for their ability to ferment. Some notable differences are that *S. pombe* is naturally a haploid in the wild[23,24], while *S. cerevisiae* is usually found as a diploid[25,26]. This could affect the effectiveness of selection because mutations can be recessive in diploids. Therefore, the extant genome might have 'footprints' of this accumulated genetic load in *S. cerevisiae*[3,27]. Supporting this, heterosis has been observed in yeast from crosses of wild budding yeast strains[28,29]. Further, *S. cerevisiae* is within the clade of yeasts that have undergone the so-called 'whole-genome duplication event', which is thought to have profoundly shaped their metabolism due to functional divergence in paralogous gene copies[30]. Another major difference is that *S. pombe* cannot survive the loss of its mitochondrial DNA and relies on oxidative phosphorylation for growth, i.e. it is petite-negative, while *S. cerevisiae* can survive without mitochondrial DNA, i.e. it is petite-positive, highlighting a rare ability of budding yeast [31–33]. Thus, domestication, competition with other microorganisms, and exploration of poorly oxygenated niches might have led *S. cerevisiae* to produce and process ethanol more efficiently than *S. pombe* [34,35]. Therefore, their different life cycles and evolutionary histories could lead them to different evolutionary outcomes

Hints of the effects of contrasting life and evolutionary histories on evolutionary signatures emerge when comparing the molecular processes that are under selection and could potentially allow for the prediction of molecular evolution that may occur during experimental evolution. For example, *S. cerevisiae* gene content variation across strains is more frequent than in *S. pombe*, and loss-of-function (LOF) mutations, such as nonsense mutations and frameshift deletions, tend to be recurrently fixed across populations[36]. The rate of copy number variants (CNV) is also higher in the budding yeast sub-telomeric regions and can contribute to its adaptation[36]. Additionally, although *S. pombe* has a similar substitution rate to the budding yeast, it has a higher indel mutation rate with a bias toward insertions[37]. Previous genomic analyses also showed that 43% of *S. pombe* genes have introns compared to 5% in *S. cerevisiae* and upstream intergenic regions are larger in the former[38]. The difference in extent of non-coding regions is also present at the whole-genome level: annotated coding regions span around 70% of *S. cerevisiae* genome compared to 60% for *S. pombe*[39–41]. It is currently unknown if this implies that *S. pombe* would preferably adapt through regulatory changes while *S. cerevisiae* would do so through gene content changes and mutations in protein-coding genes. However, the mutations in the non-coding regions of *S. pombe* are known to be involved in transcription regulation and should affect trait evolution and adaptation[42]. Thus, comparing the evolutionary processes and targets of adaptation in *S. cerevisiae* and *S. pombe* through experimental evolution could help highlight factors explaining differences in evolutionary outcomes across and within species.

To address the gap in understanding how species with similar gene content, but different life histories, might evolve in the same environment, we undertook a laboratory evolution experiment where we founded about 16 populations, each of 5 different budding yeast species, as well as the *S. pombe* fission yeast. Here, we describe the dynamics and molecular evolution of the fission yeast populations over the first 10,000 generations. Fission yeast is considered the outgroup of this set of species, and so it serves as a useful anchor for expectations within our chosen fungal phylum. We analyze the mutational spectrum, the molecular evolutionary dynamics, and identify, through pathway enrichment analysis and whole transcriptome sequencing, a case of parallel evolution where *S. pombe* populations have rewired their central carbon metabolism to reduce dependency on oxygen, which mirrors similar events in wild *S. pombe* populations and in related *Schizosaccharomyces*[32,35,35,43,44].

## RESULTS

### Contrasting fitness gain of fission yeast during 10,000 generations of evolution

To compare the evolutionary processes contributing to adaptation and selection targets between *S. pombe* and *S. cerevisiae*, we founded 15 *S. pombe* populations and performed experimental evolution for 10,000 generations, collecting and freezing samples approximately every 70 generations in 27% glycerol (**Methods; Fig. 1**). The populations were all founded from single colonies of the same *S. pombe* haploid laboratory strain (972h-) and serially propagated in batch culture in one well of a lidded, unshaken flat-bottom 96-well plate in rich media at 30°C with a daily $1{:}2^{10}$ dilution. 5 populations were lost during the first 10,000 generations of evolution, due to contamination or mechanical pipetting errors. Because of the plate lidding and the absence of shaking, these conditions correspond to a high-sugar hypoxic environment. The media and temperature are also identical to our previous experimental evolution study, which analyzed 10,000 generations of evolution for *S. cerevisiae* populations that were passaged simultaneously using liquid handling robotics[3]. Although these growing conditions may be sub-optimal for growth of *S. pombe* and so the selection pressure faced by the species may differ, our experiment allows us to control for some of the environmental variate for the comparison of evolutionary outcome.

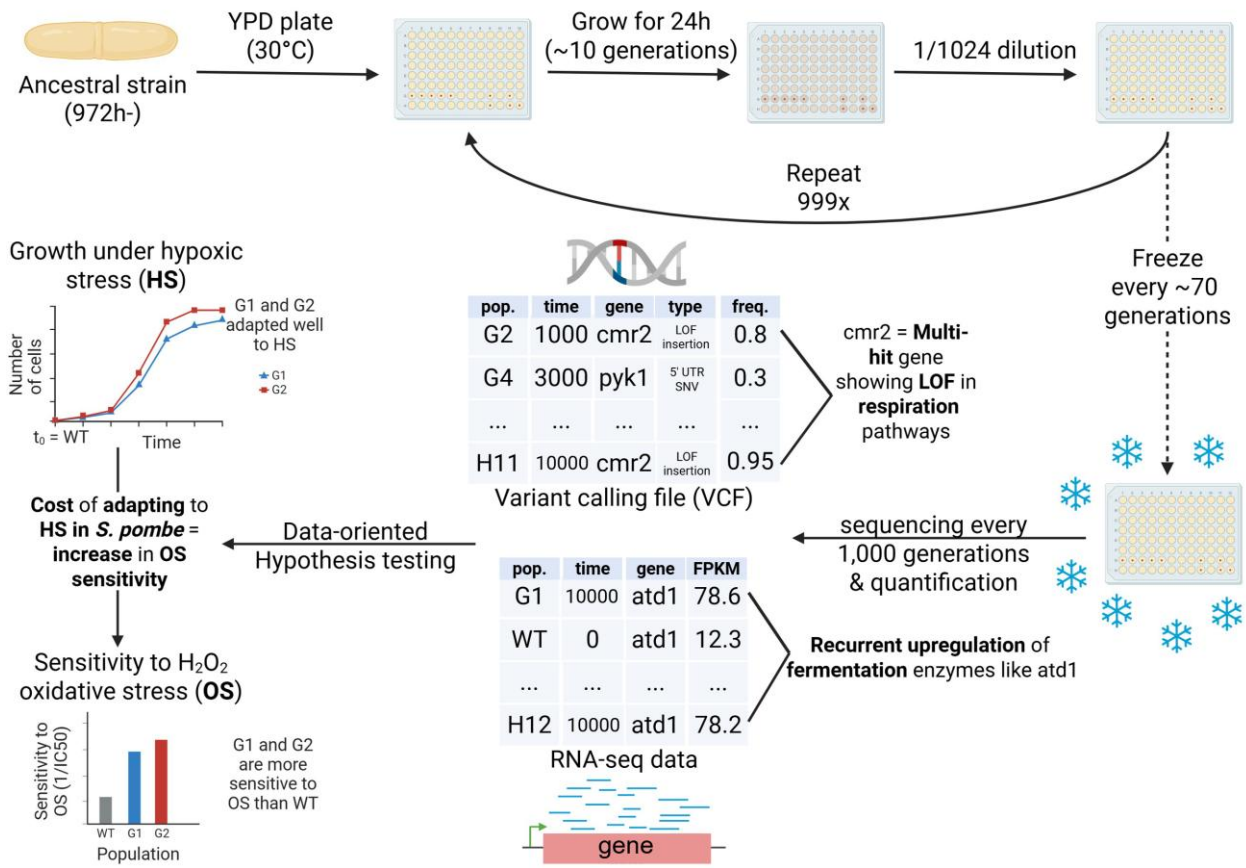


**Figure 1 Experimental approach.** We evolved 15 *S. pombe* populations at 30°C in lidded YPD 96-well plates for 10,000 generations, collecting and freezing samples approximately every 70 generations in 27% glycerol at -80 °C and sequenced them every 1,000 generations. These populations were part of a larger experimental evolution project, which explains why they occupy two rows of the 96-well plates and were examined regularly for contamination (**Methods**). Because the experimental conditions yielded a doubling rate of 10 generations per day, we performed a 1/1024 serial dilution every day ($1/2^{10}$), which can be done by two consecutive 1:32 dilutions with 96-well plates. This yielded ~100 time points or samples from which we sequenced DNA to identify variants. We also sequenced RNA at the initial (WT) and final time points to quantify gene expression changes. To find targets of selection at the genomic levels, we identified multi-hit genes, i.e. the genes that were recurrently hit by fixed mutations (frequency >= 75%) that are not synonymous (indels, missense, or nonsense) in multiple populations. At the transcriptomic level, we identified genes that were differentially expressed across several evolved populations compared to WT or to populations not exhibiting a change in a phenotype of interest, e.g. sensitivity to oxidative stress (OS). These data allowed us to generate hypotheses about adaptation in the 10 populations surviving, i.e. G1-G5, G9, H9 and H11-12, which we tested experimentally. For instance, in the figure, G1 (blue) and G2 (red) both adapts to hypoxic stress (HS) at the cost of becoming more sensitive to OS.

To determine whether the evolved populations adapted to these conditions, we measured the fitness at the initial and final time points. We serially propagated each population and the ancestral strain separately in a mixture with a *S. cerevisiae* reference strain expressing green

fluorescent protein (GFP) for 3 days. We used a flow cytometer to measure the frequency of the dark *S. pombe* populations and the green *S. cerevisiae* strain daily, and assessed fitness based on changes in frequency (**Equation 1 in Methods**). The evolved populations are all fitter than the ancestral strain (**Supplementary Fig. 1**) as observed in other experimental evolution studies[3,6]. However, the fitness gains of the *S. pombe* lineages after 10,000 generations of evolution are significantly smaller than those of *S. cerevisiae*'s haploid populations in a similar rich-media hypoxic environment (**Supplementary Fig. 1**). This slower rate of fitness gain is not due to *S. pombe* being 'pre-adapted' to this environment, as the ancestor *S. cerevisiae* strain used in a previous study is much fitter than the ancestor *S. pombe* strain used here. We presume that this is the result of *S. cerevisiae* having higher glycolytic and fermentation rates and being able to more readily adapt to the experimental conditions through a more diverse set of stress response pathways as a result of having explored many anaerobic niches throughout its evolutionary history[32,34,35,45]. *S. pombe*, on the other hand, is a poor fermenter in anaerobic conditions[32] and has a less robust hypoxic stress response[46]. Together, these factors may partly explain differences in adaptation rates under the same environmental conditions, as each species may evolve through different adaptation strategies with different associated costs.

**Differences in the genome architecture partially explain the different mutation spectra of *S. pombe* and *S. cerevisiae***

To uncover potential differences in adaptation strategies between the two species and the molecular mechanisms underlying them in the evolved populations, we performed whole-population, whole-genome sequencing every 1,000 generations on the 10 *S. pombe* populations. We successfully grew cells from 93 out of the 100 corresponding stored samples and sequenced these time points using Illumina NovaSeq paired-end sequencing (mean coverage ~40X). The remaining 7 time points were presumably lost during storage and were not associated to any specific population or particular archival date. We then called single-nucleotide variants (SNVs) and indels using Varscan2.4.6[47]. Because contamination, sequencing errors and low-complexity regions can introduce variant calling errors, we applied some filters to the called variants [48,49] while leveraging the time series for call consistency (**Methods**).

To validate the accuracy of the called variants, we measured the substitution rates and fixed indel bias, e.g., the fixed insertion-to-deletion ratios, in each *S. pombe* population. We measured a fixed insertion-to-deletion ratio ranging from 2.11 to 6.33 (median = 4.43, $\mu$= 4.32, and $\sigma$= 1.22; **Supplementary Fig. 2**), which is consistent with the insertion preference observed in previous *S. pombe* genomic analyses [37]. As for the substitution rate, we measured an average of 1.91E-10 fixed substitutions per site per generation (median = 1.72E-10, $\sigma$= 6.76E-11), which is similar to results from mutation accumulation experiments in *S. pombe* (2.00E-10 in Farlow et al. 2015) and within the range of *S. cerevisiae*'s substitution rate estimates (1.67 ± 0.04E-10 in Zhu et al. 2014 and 3.30± 0.80E-10 in Lynch et al. 2008)[37,50,51].

Although both species accumulate substitutions at a similar rate, their genome architectures differ. *S. cerevisiae* is a domesticated post-WGD yeast species, contrary to *S. pombe* [52–55].

229 Furthermore, the extent of coding regions in *S. pombe*'s genome (~60%) is smaller than in *S.*
230 *cerevisiae* (~70%) [34,37,56,57]. Under a null model of evolution in which all loci have the same chance
231 of being hit by substitutions, the differences in the mutation spectra of these species should reflect
232 the differences in genome architecture. Deviations from this expectation would suggest the
233 presence of selection in certain loci and a preference for specific types of mutations. Thus, we
234 compared the frequency of different variants observed in the 10 *S. pombe* haploid populations to
235 the one observed in *S. cerevisiae* haploid populations' experimental evolution[3] (**Fig. 2A**).

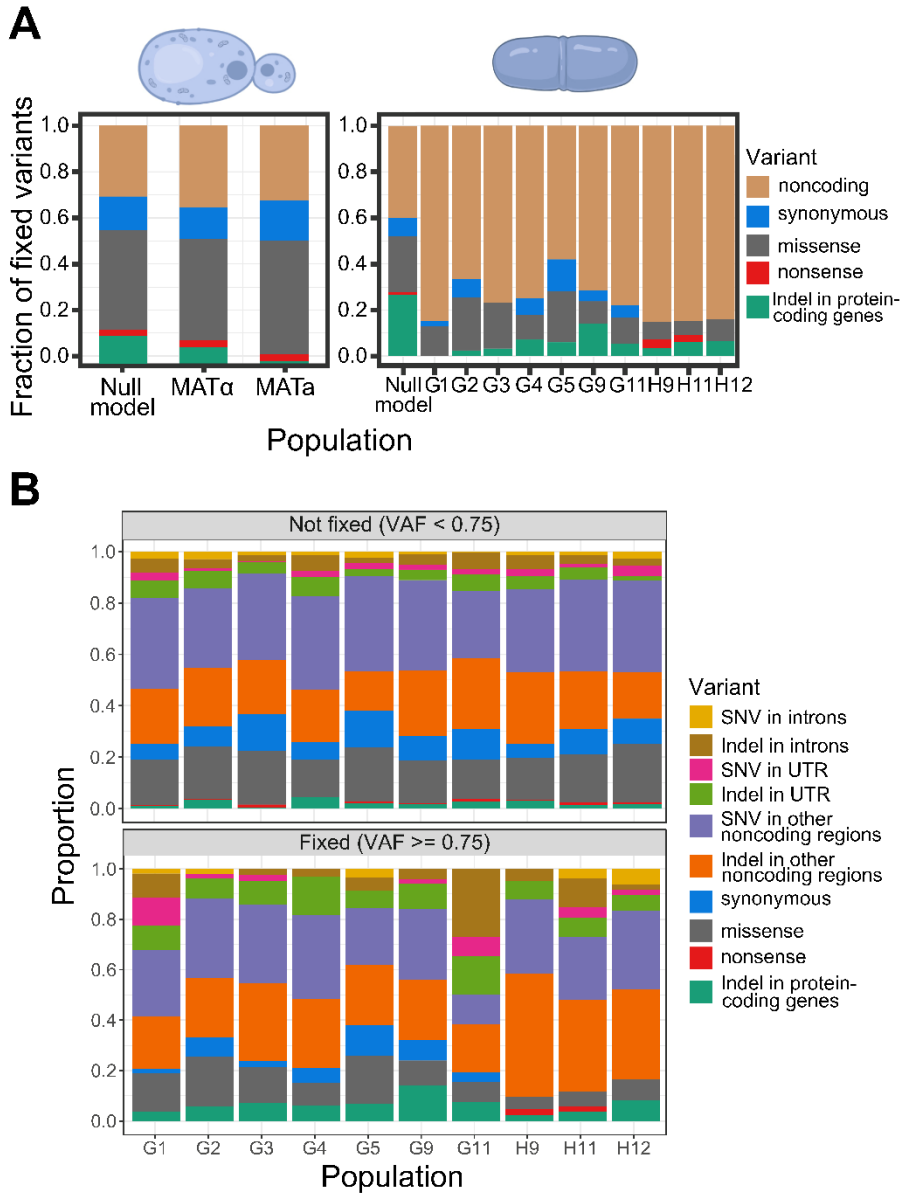


236 **Figure 2 Comparison of the fixed variant spectra between the budding and the fission yeasts**
237 **and the fixation bias in *S. pombe* evolved populations.** A) The fixed variant (allele frequency
238 >= 75%) spectrum in *S. cerevisiae*'s haploid populations after 10,000 generations of experimental
239 evolution (left, data from Johnson et al. 2021) compared to *S. pombe*'s (right). The experimental
240 evolution protocol is the same for both species and is described in Johnson et al. 2021[3]. The null
241 model is obtained by calculating the expected number of fixed variants in each category based on

242 the species' evolution rate, genome size, genome architecture, and the proportion of single-
243 nucleotide mutations derived from the genetic code and associated with a specific category of
244 protein-coding region mutations (**Equations 2 and 3 in Methods**). B) The upper part of this panel
245 represents non-fixed variants, while the bottom part represents the fixed variants in each of the 10
246 evolved *S. pombe* populations.

247 The fixation of variants in the noncoding regions of *S. pombe* is higher than expected by the null
248 model, suggesting the predominance of positive selection in noncoding regions or purifying
249 selection in coding regions. The fission yeast populations mainly evolved through mutations in
250 non-coding regions with a bias toward fixing indels and not fixing coding regions SNVs (**Fig. 2B**),
251 which is different than what has been reported for the budding yeast[3]. To test if the stronger fixation
252 bias of indels in non-coding regions compared to protein-coding genes reflects a signal of purifying
253 selection in protein-coding genes, we compared the indel rate, i.e., the number of indels per kb,
254 based on whether the indel locus is coding or non-coding and whether the indel changes the DNA
255 reading frame or not (**Supplementary Fig. 3**). In protein-coding genes, controlling for increased
256 likelihood of shorter indels, we find that indels that do not cause frameshifts are enriched compared
257 to the ones that do (**Supplementary Fig. 3**). In contrast, indels in non-coding regions do not exhibit
258 such selective constraints on their length. This is similar to the observed frequencies of
259 polymorphisms in humans and budding yeast[58] and suggests stronger purifying selection in
260 protein-coding genes. This and the paucity of fixed coding mutations compared to *S. cerevisiae*
261 populations suggest that the genetic context of *S. pombe* is less amenable to tinkering through loss-
262 of-function mutations. One hypothesis for this may be that the whole-genome duplication event in
263 *S. cerevisiae* provided more genetic redundancy, which has been suggested to increase evolvability
264 through coding mutations or through rapid changes in functional gene content[30,59] (see Discussion).
265 An additional explanation is that *S. pombe* has a much higher essential gene load than S. cerevisiae
266 (26.1% vs 17.8%)[60]. Altogether, these results show that the differences in the mutation spectra of
267 *S. cerevisiae* and *S. pombe* are only partially explained by their genome architectures, revealing
268 signatures of selection in both coding and non-coding regions.

269 **The genomic targets of adaptation in *S. pombe* are genes involved in the response to hypoxic**
270 **and oxidative stresses**

271 Although the *S. pombe* mutation spectrum revealed a signal of purifying selection in protein-
272 coding genes, we cannot exclude the presence of loci evolving under positive selection. However,
273 we may expect the targets of adaptation to vary between fission and budding yeasts due to
274 differences in their evolutionary histories and genetic architectures. To detect such loci in 205 *S.*
275 *cerevisiae* populations, Johnson et al. (2021) looked for signals of convergent evolution. More
276 precisely, they defined a "hit" as a fixed variant that is not synonymous (missense, nonsense and
277 indels), and a multi-hit gene as a gene having hits in multiple populations. This enabled the
278 identification of 1,092 genes with hits in at least 3 out of 205 populations. Among these genes,
279 they identified a set of 189 genes with hits in at least 6 populations that were enriched in functions
280 related to the adenine biosynthesis pathway, the mating pathway, and negative regulators of the
281 Ras pathway. These signals of parallelism at the levels of biosynthetic and signaling pathways
282 were driven by LOF mutations, which were primarily frameshift deletions and nonsense mutations.

283 Using the same approach with a minimum threshold of 2 out of 10 populations in which a
284 gene has a hit, we identified 19 multi-hit genes with hits in either the cis-regulatory region or the
285 coding region (**Table 1**), which is comparable to what was expected from resampling fixed variants
286 from our previously studied *S. cerevisiae* populations (19 observed vs 23.8 expected, p-value =
287 0.15, one-tailed test), indicating a comparable signature of parallelism.

| **Gene symbol/ systematic ID (Number of populations with a hit (PH))** | **Function(s) (biological process)** | **Gene category (Link with the response to HS and OS)** | **Characterization of the hit(s) (Gene product truncation or potential LOF)** |
|---|---|---|---|
| ***bmc1*/ SPBC2A9.10** (2) | Bin3 family RNA methyltransferase (snRNA metabolic process) | Others | • 1 frameshift insertion in both G1 and G3 (Truncation of 14 out of 268 residues) |
| ***bop1*/ SPAP32A8.03c** (2) | ubiquitin-protein ligase E3 (protein degradation) | HS-related (Ubiquitin-dependent protein degradation is ATP-dependent[61,62]. The response to HS requires specific E3 ligases that activate sterol regulatory elements (SRE) and the decrease of the activity of other E3 ligases that do not contribute to the HS response, e.g. Ubr1[63–65]) | • 1 frameshift insertion in both G11 and H12 (Truncation of 475 out of 513 residues) |
| ***clg1*/ SPBC1D7.03** (2) | Cyclin-like protein involved in autophagy (signaling, molecular activity regulation and autophagy) | HS- and OS-related (in *S. pombe*, *clg1* regulates autophagy[66]. Autophagy plays an important role in the response to | • 1 indel in the 5'UTR of the populations G2 and G3 |

| | | | |
|---|---|---|---|
| | | HS and OS by recycling biomolecules and removing damaged cell components[67,68]) | |
| ***cmr2/* SPAC56F8.02** (2) | acetyl-CoA biosynthesis (respiration) | HS- and OS-related (Acteyl-CoA is involved in the first step of the TCA cycle and respiration enzymes are involved in energy production and ROS removal[69]) | • 1 missense mutation in the AMP-dependent synthetase/ligase domain[40] in G1<br>• 1 nonsense SNP in H11 (Truncation of 174 amino acid residues in the Dip2-like domain[40] out of 1517 protein residues) |
| ***ctf18/* SPBC902.02c** (4) | Ctf18 RFC-like complex subunit Ctf18 (DNA replication) | HS-related (Upregulated under HS[67]) | • 1 indel in the first intron of the gene in the populations G3, G5, H9, and H11 |
| ***dep1/* SPBC21C3.02c** (2) | Rpd3L histone deacetylase complex subunit (chromatin organization and transcription regulation) | HS-related (Upregulated under HS[67]. *dep1Δ* strain is more sensitive to hydrogen peroxide[70] than WT) | • 1 indel in 3'UTR in the populations G2 and G11 |
| ***fet4/* SPBP26C9.03c** (2) | plasma membrane iron/zinc ion transmembrane transporter (inorganic ion homeostasis and transmembrane transport) | HS- and OS-related (Iron cofactors support major biochemical processes like the heme biosynthesis, TCA cycle, electron transport chain, translation, and DNA repair[71]) | • 1 indel in 5'UTR in the populations G2 and H11 |
| ***fhn1/* SPBC1685.13** | Eisosome assembly protein | HS-related (Upregulated | • 1 indel in 3'UTR in the populations G3 and H11. |

| | | | |
|---|---|---|---|
| (3) | (membrane organization) | during the response to hydrogen peroxide[72]) | 1 indel in 3'UTR in the populations G9 |
| ***iss9/* SPBC2A9.11c** (2) | SAC3/GANP/THP3 family protein (transcription or RNA surveillance) | Others | • 1 frameshift insertion in the populations G1 and G5 (Truncation of 315 out of 395 residues) |
| ***pfl2* SPAPB15E9.01c** (3) | cell surface glycoprotein, flocculin Pfl2 (cell adhesion) | HS- and OS-related (Flocculation and adhesion enhance survival by protecting against stressful conditions[73,74]) | • 5 missense hits in G3: chrI_A3989282G (R->G), chrI_G3989285A (A->T), chrI_G3989294A (G->S), chrI_G3989384A (G->S), chrI_G3989390A (A->T)<br>4 missense hits in G5: chrI_G3989877C (R->T), chrI_G3989879A (G->R), chrI_A3989878T (R->S), chrI_G3989877C (R->T)<br>*Pfl2 is a disordered protein so it has many S, R and T residues[40,75]<br>• 2 indels in 5'UTR in the populations G1 and G5 |
| ***pfl5/* SPBC1289.15** (3) | cell surface glycoprotein, flocculin Pfl5 (cell adhesion) | HS- and OS-related (Flocculation and adhesion enhance survival by protecting against stressful conditions[73,74]) | • 2 Y→F missense hits in G2 and H12 around the middle of the protein. 1 K→E missense hit in G5<br>• The same frameshift insertion in the populations G2 and H12 (Truncation of 518 out of 1283 residues around the middle of the protein).<br>1 deletion in G2 (Truncation of 528 out of 1283 residues around the middle of the protein) |
| ***pof15/* SPAPB1A10.14** (2) | Ubiquitin complex adaptor; F-box protein (protein degradation) | HS-related (Downregulated under HS[67,76]. Ubiquitin-dependent protein degradation is | • 1 N→D missense hit in G5<br>• 1 frameshift deletion in the population H12 (Truncation of 135 out of 243 residues) |

| | | | |
|---|---|---|---|
| | | ATP-dependent [61,62]) | |
| ***pqr1/* SPAC6B12.07c** (3) | SPX-RING-type ubiquitin-protein ligase regulating phosphate transport and homeostasis (protein degradation and transmembrane transport) | HS-related (Upregulated during the response to hydrogen peroxide[72]. Excess of intracellular phosphate and polyphosphate is associated with improper autophagy-dependent proteolysis in vacuoles[77]) | • 1 SNV in 3'UTR in G9, G11 and H11 |
| ***prr1/* SPAC8C9.14** (2) | stress-responsive DNA-binding transcription factor Prr1 (transcription regulation and response to oxidative stress) | OS-related (*prr1* is a positive regulator of the OS response. It binds *pap1* as part of a positive regulation of transcription, and it regulates *ctt1*, *srx1*, *trr1* during the cellular response to OS[78,79]) | • 1 P→Q missense hit in the signal transduction response regulator/receiver domain in H12<br>• 1 frameshift insertion in the population H11 (Truncation of 517 out of 540 residues) |
| ***pyk1/* SPAC4H3.10c** (5) | pyruvate kinase (carbohydrate metabolic process) | HS- and OS-related (The gene product catalyzes the last step of glycolysis. This influences the fermentation-respiration balance and thus biomass production and stress resistance[35]) | • 1 missense hit V→L in the barrel domain in H11<br>• 2 SNVs in 3' UTR in G1<br>• 1 SNV in 3' UTR in H12<br>• 1 deletion in the promoter (5' UTR) in G3<br>• 1 deletion in 5' UTR in G4 |

| | | | |
|---|---|---|---|
| ***pzh1/* SPAC57A7.08** (2) | serine/threonine protein phosphatase (signaling) | HS- and OS-related (*pzh1* is a positive regulator of the response to OS[80]. It is also upregulated under HS[67]) | • 1 deletion of 2 residues (positions 73 and 74) in the N-terminal disordered region[40] in both G5 and G9 |
| ***rpp1/* SPAC3A12.04c** (2) | RNase P and RNase MRP subunit p30 (ribosome biogenesis and tRNA metabolic process) | Others | • 1 SNV in the fourth intron of the gene in populations H11 and H12 |
| ***seb1/* SPAC222.09** (2) | poly(A)site selection protein (mRNA metabolic process and snoRNA metabolic process) | Others | • 1 missense T→I hit in the RNA recognition motif domain in G1<br>• 1 missense K→N hit in the CTD-interacting domain in G2 |
| ***ubp9/* SPBC1703.12** (2) | ubiquitin C-terminal hydrolase Ubp9 (protein degradation and vesicle-mediated transport) | HS- and OS-related (*ubp9Δ* strain is more sensitive to hydrogen peroxide[70]. Protein degradation and vesicle-mediated transport enable the recycling of biomolecules under stress conditions[61,62]) | • 1 frameshift insertion in the populations G3 and G9 (Truncation of 265 out of 585 residues, including most of the ubiquitin carboxyl-terminal hydrolase domain) |

**Table 1 Multi-hit genes and their LOF mutations.** The gene annotations are based on Pombase data[40].

The presence of hits in multi-hit genes was more recurrent than expected under a null model where variants are fixed at the same rate across all the genes (**Methods**; Two-sided Wilcoxon rank sum p-value < 0.05; **Supplementary Fig. 4**). This signal of positive selection is also consistent with the fixation of these hits (**Fig. 3**) and the fixation of the same hit at different times in multiple populations (**Table 1**; **Fig. 3**).

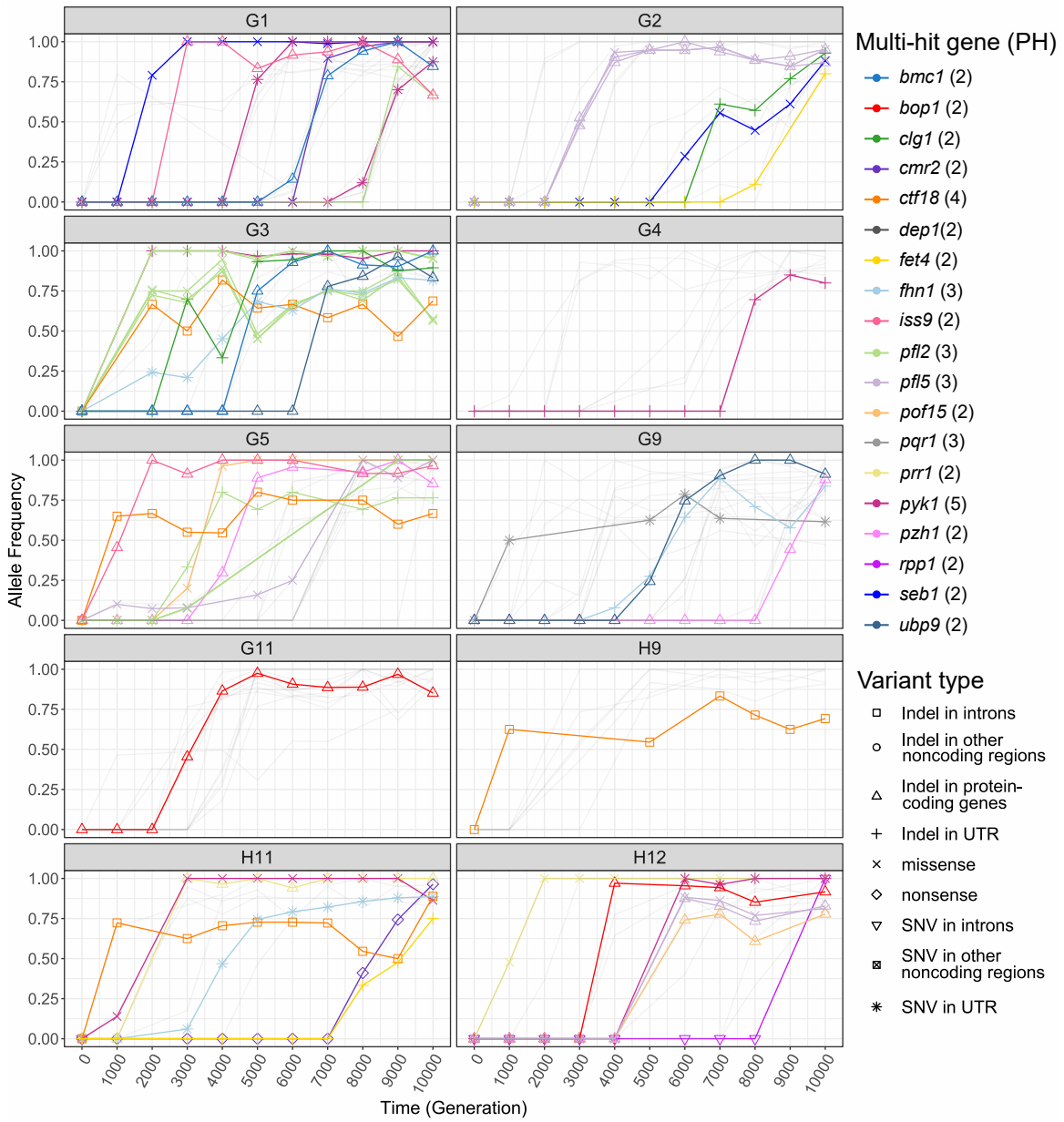


**Figure 3 Time series of the hits' allele frequencies in evolved *S. pombe* populations and multi-hit genes.** Time series of the hits' allele frequencies in the *S. pombe* populations. We defined a "hit" as a fixed variant that is not synonymous (missense, nonsense and indels) and a multi-hit gene as a gene having hits in multiple populations. In each population, variants that were never fixed or that are not located in multi-hit genes are represented by more transparent lines. In the legend, PH represents the number of populations in which the gene is hit.

We also found evidence for adaptation through LOF mutations in the 10 evolved *S. pombe* populations, although these mutations are primarily frameshift insertions rather than deletions. This is consistent with a different indel bias than in *S. cerevisiae*[3] (**Table 1; Fig. 2**) and a preference for insertion, which we previously highlighted (**Supplementary Fig. 2**).

305 Most of the *S. pombe* multi-hit genes are involved in the response to hypoxic stress (HS)
306 and sometimes to oxidative stress (OS) (**Table 1**), which may be due to growth in an unshaken
307 and lidded environment. Adapting to HS requires compensating for the energy deficit caused by
308 respiration deficiency through fermentation and removing the associated reactive oxygen species
309 (ROS)[32]. Further, the increase in ethanol production through fermentation can decrease lipid
310 membrane integrity. This includes the mitochondrial membrane, which harbors the electron
311 transport chain and antioxidant components that stabilize ROS through electron transfer. Thus, the
312 increase in fermentation in hypoxic conditions can lead to ROS production through electron
313 leakage[45]. This is consistent with fixed mutations in genes involved in the removal of damaged
314 cell components and ROS like *clg1*, *pqr1*, *pzh1* and *ubp9*. Fermentation is also known to yield
315 smaller energy and biomass outputs than respiration [32,34], which can affect the synthesis of redox
316 metabolism components. Finally, *S. pombe* is known to be sensitive to polypeptones included in
317 the growth media of the experiment (due to cell lysis), and it is thought that the respiratory
318 Coenzyme Q (CoQ10) plays a role in promoting this trait[81,82]. Under the same conditions, *S.*
319 *cerevisiae*, being petite-positive, can rely on fermentation along with a robust antioxidant response
320 to mitigate the ROS produced by fermentation and hypoxic stress[45], which may explain why such
321 mutations are not typically observed in budding yeast experimental evolution studies.

322 Another piece of evidence supporting the importance of energy- and ROS-related processes
323 in this environment is the fact that the strongest signal of convergent evolution is in the lower
324 glycolysis gene *pyk1*, which had fixed mutations in 5 populations. This gene encodes for the
325 enzyme involved in the synthesis of pyruvate, which influences respiration and fermentation as it
326 can be transformed into Acetyl-CoA or into ethanol[35]. In the population H11, the glycolytic flux
327 going towards respiration seems to be compromised by a fixed LOF mutation in *cmr2* (**Fig. 3**),
328 which encodes for the enzyme converting pyruvate into Acetyl-CoA. The fixation of this LOF
329 mutation might be related to a benefit in re-orienting the glycolytic flux mostly towards
330 fermentation. In the same population, we also observed the fixation of a LOF mutation in *prr1*,
331 which encodes a transcription factor involved in the response to OS. Because *prr1* is not known to
332 be directly activated by HS, there might be other OS response genes involved in ROS removal
333 under HS, and *prr1* might not be needed unless ROS levels exceed the removal capabilities of
334 these genes. For instance, in *S. pombe,* the transcription factor Sre1 is activated under low oxygen
335 levels and activates genes involved in ROS removal or protein catabolism like *ccs1* and
336 *SPAC23C11.06c*[67,83]. The benefit of inactivating *prr1* while respiration is limited under HS might
337 thus be related to conserving energy and cell resources. However, losing such response regulators
338 and relying on fermentation may make *S. pombe* more sensitive to OS.

339 **Most evolved *S. pombe* populations are more sensitive to oxidative stress**

340 As we observed fixed LOF mutations in genes modulating OS response and the glycolytic flux
341 towards respiration, we hypothesized that evolved populations might be more sensitive to OS.
342 Populations adapting to hypoxic stress or to polypeptone-mediated lysis may exhibit decreased
343 respiration rates, resulting in reduced energy and biomass production[32]. This could affect the
344 synthesis of the components of the redox metabolism, e.g. glutathione (GSH) and ubiquinone
345 (CoQ10)[69,84]. These enzymes and the ones involved in the respiratory chain rely on the biomass

346 produced by glycolysis and the TCA cycle as well as ions like iron and sulfur for their
347 functions[32,84–86]. Consistent with this, we observed the presence of hits in the iron transporter *fet4*
348 in multiple populations, which may compensate for respiration deficiency. Indeed, iron can help
349 capture or transport the low amount of oxygen available, and iron is a critical component of the
350 respiratory chain enzymes. Moreover, one *S. pombe* evolved population harbors a LOF insertion
351 in *prr1* (**Table1**, **Fig. 3**), an important transcription factor involved in the response to oxidative
352 stress[79]. As *prr1* activates the catalase *ctt1*, the sulfiredoxin *srx1*, and the thioredoxin *trr1*[78], a fixed
353 LOF mutation in this gene suggests that evolving under HS can decrease *S. pombe*'s ability to
354 manage OS, which is consistent with observations in the cousin species *S. japonicus*[32]. These
355 species likely rely on fermentation to adapt to hypoxic conditions, which may expose them to more
356 ROS[45]. Altogether, these observations led us to believe that the evolved *S. pombe* populations are
357 more sensitive to OS than WT as a result of their adaptation to HS.

358 To test this, we used hydrogen peroxide as a source of oxidative stress during a growth
359 assay (**Methods**) and compared the OS sensitivity of the WT to the OS sensitivity of the 10 evolved
360 populations (**Fig. 4A**).

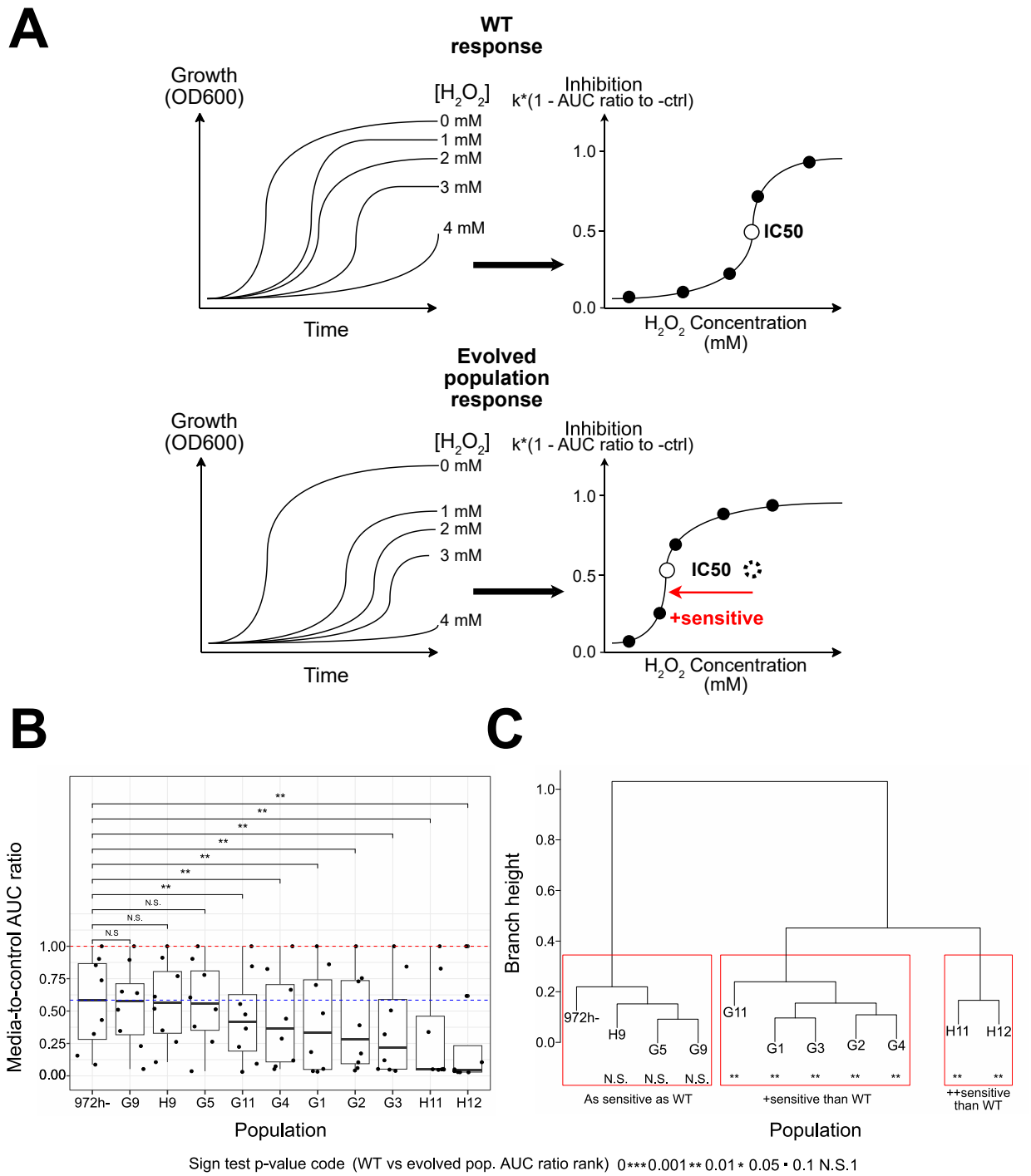


**Figure 4 Comparison of the sensitivity levels to $H_2O_2$ between *S. pombe* WT and evolved populations**. A) Schematic illustrating the expected difference in sensitivity between WT and evolved populations. We inferred the degree of inhibition at each concentration of $H_2O_2$ based on the expression in Equation 4 and the sensitivity of each population based on Dose-Response analysis (**Methods**). The IC50 recapitulates the level of sensitivity of a population to hydrogen peroxide. Lower IC50 values can be interpreted as higher sensitivity to $H_2O_2$, which is what we expected for the evolved populations. B) The ratio between the AUC of a population at a certain

368 $H_2O_2$ concentration + YPD and the AUC in YPD without $H_2O_2$. This is another metric of
369 sensitivity with an expected maximum of 1 (red dotted line). The blue dotted line represents the
370 median sensitivity of the WT. The WT AUC ratio is compared to each evolved population using a
371 sign test on the ranks. The two-sided p-values of this test are encoded as follows: *** from 0 to
372 0.001 exclusively, ** from 0.001 to 0.01 exclusively, * from 0.01 to 0.05 exclusively, "." from
373 0.05 to 0.1 exclusively and N.S. otherwise, which is the acronym of "non-significant". C) Red
374 boxes represent the population clusters, which are based on the AUC ratios.

375 The evolved populations clustered into 3 groups: 3 out of 10 populations had a similar sensitivity
376 to $H_2O_2$ as the WT, 5 out of 10 populations were more sensitive than WT, and 2 out of 10 evolved
377 populations were much more sensitive than the WT strain, including H11, the population that lost
378 the OS response regulator *prr1* (**Fig. 4B** and **4C**). This increased sensitivity to OS after adapting
379 to HS has not been observed in *S. cerevisiae*, which may be explained by contingency, i.e. more
380 exposure to anaerobic environments during its evolutionary history and a better redox
381 metabolism[32,34]. However, it is reproducible in most of the evolved *S. pombe* populations, and has
382 likewise been observed in related species, including wild *S. japonicus*[32] (see Discussion).

383 **Transcriptomics analysis reveals many genes involved in the response to HS and downstream**
384 **effects explaining the sensitivity to OS in multiple populations**

385 The sensitivity to OS developed after adapting to HS was revealed by convergent evolution at the
386 genomic level, i.e. multi-hit genes. However, identifying transcriptomic differences between more
387 sensitive and WT-like populations could help reveal genes driving this evolutionary outcome and
388 explain how point mutations and indels contribute to the evolution of these traits through
389 transcriptomic regulation. Moreover, most of the mutations in the pyruvate kinase (*pyk1*) locus are
390 located in the untranslated regions flanking the gene, which contains cis-regulatory elements
391 (CRE) like the promoter (**Supplementary Fig. 5**). Hits in these loci could explain the adaptation
392 to HS through changes in transcript levels through cis-regulatory and trans-regulatory effects[87–91].
393 These questions thus led us to investigate the role of transcriptomic changes in the responses to
394 HS and OS. To do so, we performed RNA-seq of the WT ancestor and the final evolved
395 populations, and compared the transcriptomic profiles of populations more sensitive to $H_2O_2$ than
396 WT with those of populations as sensitive as WT (**Methods**).

397 Consistent with the need to compensate for biomass and energy deficit under HS due to
398 limited respiration[32], most evolved *S. pombe* populations upregulated genes involved in heme
399 metabolism/transport, the transport of biomolecules like amino acids or hexose, lipid metabolism,
400 fermentation, and ion transport (**Fig. 5, Supplementary Table 1**).

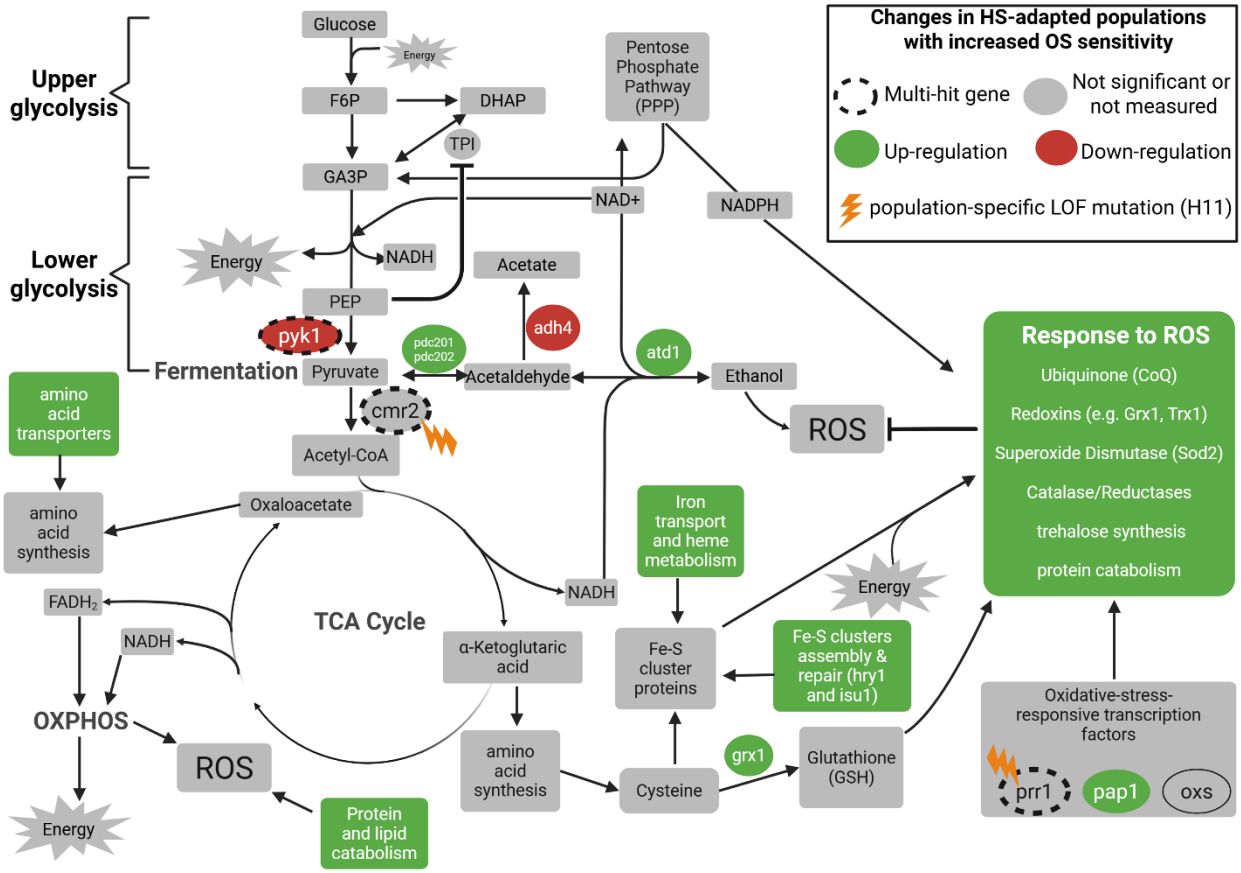


**Figure 5 Fission yeast cellular responses to hypoxic stress in populations with increased OS sensitivity.** Transcriptomic changes are determined by comparing the populations with increased OS sensitivity to populations with similar OS sensitivity than WT while genomic changes are obtained by comparing these evolved populations to WT (**Methods**). The green fill represents an upregulation while the red fill represents a downregulation. The grey fill represents molecules or processes that were not associated with a significant effect or not measured (no data). The orange lightning symbol represents LOF hits in H11, the only population with such variants in several multi-hit genes (dotted line stroke).

Another way the fission yeast populations could respond to HS is by improving the electron transport chain (ETC) to leverage the limited amount of oxygen available. The upregulation of the heme transporters *str3* and *shu1* in many evolved populations supports such a strategy (**Supplementary Table 1**). Heme can help capture and transport the small amount of oxygen available under HS and it is an essential component of the electron transport chain (ETC)[85].

Despite the presence of transcriptomic changes explaining HS adaptation and the OS sensitivity cost, most of the differentially expressed genes were different than the targets of selection identified at the genomic level, except for *pyk1*, *pzh1* and *ubp9*. For instance, the multi-hit gene *clg1*, which is a positive regulator of autophagy[40,66], is not differentially expressed between populations with different OS sensitivity, but 22 other genes involved in autophagy exhibit an expression level increase from 54.4% to 229% (**Supplementary Table 1**) and they are not mutated. Autophagy might be one of the few pathways that contribute to cross-resistance to both HS and OS by recycling biomolecules and removing damaged cell components[67,68]. This is

422 consistent with the upregulation of the multi-hit gene *pqr1*, the ubiquitin-protein ligase regulating
423 phosphate transport and homeostasis, such that autophagy is not compromised in vacuoles[77].
424 Another process linked to cross-resistance to multiple stresses is vesicular transport[92,93]. One of its
425 genes, i.e. *ubp9,* is one of the only three multi-hit genes to be differentially expressed in evolved
426 *S. pombe* populations that are more sensitive to OS than WT (log2FC = 0.885; FDR<0.05),
427 suggesting a moderate but significant link between vesicular transport and adaptation
428 (**Supplementary Table 1)**. As for the multi-hit gene *pyk1*, it is downregulated by 36.5% in
429 populations with increased OS sensitivity (FDR<0.05; **Supplementary Fig. 6**). Adaptation to HS
430 may require decreasing the glycolytic flux allocated to respiration[32] and change the
431 respiration/fermentation balance. This is consistent with the decrease of Acetyl-CoA synthesis
432 through the downregulation of the Acetyl-CoA ligase *pcs60* (53.7% decrease; FDR<0.05) and
433 selected LOF mutations in *cmr2*, which may trigger the ETC optimization responses previously
434 described as a compensatory mechanism. Similar to mutations observed in *S. japonicus*, the LOF
435 mutations in lower glycolysis and Acetyl-CoA synthesis might also contribute to OS sensitivity in
436 *S. pombe* as it would decrease the biomass and energy output of respiration, which is used for the
437 synthesis of redox metabolism proteins[69,84]. The last differentially expressed multi-hit gene is *pzh1*
438 (log2FC = 0.752; FDR<0.05), which regulates the activity of the plasma membrane H+-ATPase[94].
439 This is consistent with the need to increase energy production to compensate for respiration
440 deficiency in hypoxic conditions.
441 Apart from these three multi-hit genes, transcriptomic changes shared by populations with
442 increased OS sensitivity involved genes that were not mutated at the genomic level
443 (**Supplementary Table 1; Table 1**). This is the case for many upregulated genes involved in
444 fermentation, e.g. *pdc201/202* and *atd1*, and in the synthesis of ETC components and their iron-
445 sulfur clusters, e.g. *cbp3-4, cbp6, coq9, sdh3, sdh8*, *qcr7-10*, *fxn1* and *isu1*. The lack of overlap
446 between selection targets at the genomic and transcriptomic levels suggests that the overall
447 changes in expression levels shared by many evolved populations are driven by trans-regulatory
448 rather than by cis-regulatory effects.

449 **DISCUSSION**

450 Over short periods of time, experimental evolution is a powerful tool to decipher molecular
451 pathways under selective constraints[3,11]. An important result from studies exploiting asexual
452 laboratory evolution is that evolution is usually not limited by mutation: adaptation usually
453 proceeds rapidly and is often dominated by large-effect mutations. In many cases, gene content
454 variation can occur (via ploidy changes), and mutations frequently inactivate gene function.
455 Perhaps the most interesting result from many of these studies is that laboratory evolution can
456 frequently recapitulate evolutionary outcomes from wild, uncontrolled evolution. Whole-genome
457 duplication, loss-of-function mutations, the rise of mutators, stable co-existence, and like here the
458 change of carbon flow towards increased fermentation, are all phenomena thought to have
459 occurred in various species at various times during their evolutionary history, but also notably in
460 cancer cells[11,95–97]. The fact that cancer cells are also evolving populations suggests that
461 experimental evolution in different single-cell organisms can reveal fundamental principles of the
462 molecular basis of adaptation. For instance, the pervasiveness of parallel evolution in the tree of
463 life could be explained by deep conservation of interconnected biological pathways.

464 Our study extends the discovery of shared molecular mechanisms of adaptation across scales in
465 diverse biological systems. For instance, *S. pombe* shares a distinct preference for insertions as a
466 mutational bias with *C. elegans*[38,]. On specific selection targets, mutations that lead to upregulation
467 of iron metabolism, autophagy regulators and vesicle transporters, and that lead to rewiring of the
468 glycolytic flux are common observations in populations adapting under iron and oxygen
469 limitation[99,100] (such as tumors). The fact that the orthologs *pykF* and *pyk1* in *E. coli* and *S. pombe*,
470 respectively, are both recurrently hit across multiple populations illustrates the conservation of
471 some selection targets at the gene level, even across distant species. Finally, parallel evolution
472 within model systems is frequent and has been observed in nearly all experimental evolution
473 studies to date, but the precise observed trait under selection varies (examples in [6,101] and reviewed
474 in[102]).

475 Despite all these common evolutionary mechanisms and outcomes, disparities can arise
476 due to differences in genome architecture and contingency. One of the major findings in
477 evolutionary dynamics is that low-fitness populations typically adapt faster than high-fitness
478 populations. This observation has been seen in several species, and in several environmental
479 contexts[3,6,11]. In the evolution environment of our study, the 'ancestor' *S. cerevisiae* is much fitter
480 than its *S. pombe* counterpart. Yet, the fitness gains by our *S. pombe* populations are relatively
481 modest (**Supplementary Fig. 1**). We propose that one explanation for this 'evolvability' is the
482 effect that we set out to study in the first place, which is evolutionary contingency. Indeed, in a
483 previous study, it was found that the identity of specific molecular pathways of gene deletions had
484 a strong impact on fitness gain after evolution[13].

485 Further supporting this, the most frequent targets of adaptation in the past *S. cerevisiae*
486 study were genes involved in adenine biosynthesis and the mating pathway, for which genomic
487 hits have high fitness effects[3]. However, these pathways are not targets of selection in these *S.*
488 *pombe* populations. Based on our understanding of the adenine biosynthetic pathways in both
489 species, mutations in adenine biosynthesis genes were not expected in our *S. pombe* populations
490 (which are ade+). In contrast, the *S. cerevisiae* populations were *ade2*-, which led them to
491 accumulate a toxic intermediate that can be suppressed by the observed adenine pathway mutations
492 after evolution. It is well known that similar effects can be observed in *ade6*- strains of *S. pombe*[103].
493 Similarly, mutations in the mating pathway might not be observed in *S. pombe* due to its
494 preferential haploid lifestyle and its mating pathway is not active in rich media[23,24].

495 A third pathway frequently mutated in the budding yeast laboratory evolution experiment
496 is the Ras-cAMP pathway[3,8,104]. Observed loss-of-function mutations in *IRA1* or *IRA2* (but usually
497 not both), relieve inhibition of Ras and lead to PKA activation [3,105]. Activation of PKA ultimately
498 leads to increased glycolysis through phosphorylation of Pyk1[106]. Our *S. pombe* populations never
499 mutated the *IRA1/2* ortholog (*gap1*), though we note that it is a single-copy gene in the fission
500 yeast. More surprisingly though, are the mutations observed in *pyk1*. These mutations are not the
501 usual loss-of-function nonsense or frameshift mutations. Instead, most mutations were found in
502 the regulatory region of the gene, which we initially believed to be an analogous way for *S. pombe*
503 to upregulate Pyk1 activity. However, whole-transcriptome analyses suggest that these mutations
504 downregulate Pyk1 activity (**Fig. 5**). Interestingly, similar mutations leading to lower Pyk1 activity

505 have been observed in wild *S. pombe* populations and in the common laboratory strain[35],
506 suggesting that decreasing Pyk1 activity may be adaptive. In Kamrad et al. (2020), the authors
507 showed that a decrease in Pyk1 activity does not increase growth rate nor biomass, seemingly
508 contradicting the strong signature of adaptation from parallel evolution. However, the authors
509 noted that lower Pyk1 activity might be an adaptive trade-off as lower glycolytic flux increases
510 oxidative stress resistance through higher pentose-phosphate pathway flux and NADPH
511 production. Despite transcriptomic analyses showing a slight decrease in *pyk1* expression levels in
512 most evolved *S. pombe* populations, they were often more sensitive to OS than WT. This is
513 explained by the fact that during our experiment, the slightly reduced glycolytic flux is mostly
514 redirected toward fermentation, which is upregulated to compensate for the fission yeast
515 respiration deficiency in hypoxic conditions.

516 Adaptation to our growth environment has led to an increased OS sensitivity for most
517 evolved populations via multiple molecular mechanisms. First, Pyk1 activity can regulate carbon
518 flow and, like the other mutations found in the wild, can favor fermentation rather than respiration,
519 as our lidded and unshaking environment is likely to lead to hypoxic stress. Supporting this, we
520 observed adaptations to HS, including LOF in enzymes responsible for the transition between
521 glycolysis and oxidative phosphorylation, and the upregulation of the fermentation rate. This leads
522 to an increase in intracellular ROS through higher ethanol production and a deficiency in the
523 production of biomass and energy, which sustains the redox metabolism[34,45]. In our dataset, 3
524 populations in which *pyk1* is downregulated have cis-regulatory mutations around the gene, while
525 G2 is the only population in which *pyk1* is downregulated without such mutations
526 (**Supplementary Figs. 5 and 6)**. This suggests that *pyk1* downregulation can evolve more easily
527 through cis-regulatory effects, but it can also evolve through trans-regulatory effects. The effect
528 of reducing Pyk1 activity here is also consistent with the other mutations we observed that appear
529 to modulate central carbon metabolism (**Figs. 3 and 5**). Second, *S. pombe* cells are sensitive to
530 polypeptones, a major component of our environment[81]. Mutations that lower respiration and flux
531 through the mitochondrial electron transport chain have been shown to increase resistance to
532 polypeptones because this sensitivity requires CoQ10[81]. Strikingly, there is also evidence in *S.*
533 *japonicus* that lower glycolysis is frequently being rewired in natural populations[32]. This suggests
534 that adaptation to HS or polypeptones in petite-negative yeast species with relatively modest
535 fermentation rates might often come at the expense of costly carbon flow rewiring, hindering the
536 response to OS.

537 Multiple genomic variants and transcriptomic changes were involved in the apparent trade-
538 off between HS and OS, e.g. the LOF or downregulation in lower glycolysis or Acetyl-CoA
539 synthesis, the upregulation of fermentation, and the upregulation of the transport and metabolism
540 of biomolecules and ions. Among these adaptations to HS, fermentation upregulation and LOF in
541 lower glycolysis and genes involved in the response to oxidative stress such as *prr1*, explain the
542 increased sensitivity to OS. However, some genes involved in OS response, autophagy and vesicle
543 transport may contribute to cross-resistance to both stresses[92,93,107–109] and indeed we observed
544 three populations (G5, G9, and H9) with hits in those pathways that did not appear to have
545 increased OS sensitivity and those populations retain WT-like expression level of the lower
546 glycolysis pathway. This cross-resistance is also observed in other species like *K. lactis, S.*

547 *cerevisiae*, and human cancer[110–113]. In *S. pombe*, the effect of the cross-resistance pathways was
548 at times insufficient to offset the cost of adapting to HS by rewiring of the glycolytic flux toward
549 fermentation and using it as the main source of biomass and energy. The fact that this trade-off has
550 not been observed in the budding yeast may be explained by its historical exposure to multiple
551 anaerobic environments and more optimal adaptations to HS[34]. In contrast, *S. pombe* and *S.*
552 *japonicus,* for which lower glycolysis is less active compared to *S. cerevisiae*, tend to adapt to HS
553 through LOF in lower glycolysis and upregulation of fermentation and upper glycolysis[32,35].
554 Furthermore, the fact that the response to HS mostly involved transcriptomic changes in genes that
555 were not mutated in coding or flanking regulatory regions suggests that the adaptive transcriptomic
556 changes observed across populations were driven by trans-regulatory rather than cis-regulatory
557 effects. This also shows that the transcriptome, an intermediate level of organization between
558 genotype and phenotype, is a complex trait that can exhibit evolutionary parallelism.

559 Despite the potential of these observations to improve evolutionary predictions, this study
560 shows that multiple mechanisms are involved and that contingency can lead to diverse
561 evolutionary outcomes, even within a single species and under the same conditions. One way that
562 future research could better predict adaptive trajectories under stress conditions is by leveraging
563 the presence of rapid transcriptomic changes in response to a new stress independently of
564 mutations, e.g. expression plasticity. These responses could provide hints toward adaptive cellular
565 changes that could later be cemented by mutations with similar effects, as is the case in bird species
566 that explore high-altitude conditions[11,114].

567 **METHODS**

568 **Experimental evolution and sequencing**

569 We evolved 15 *S. pombe* populations of the laboratory strain 972h- at 30 °C in wells of a lidded,
570 flat-bottom 96-well plate containing 128 µl of YPD plus antibiotics (1% yeast extract, 2% peptone,
571 2% dextrose, 100 µg/mL ampicillin, 25 µg/mL tetracycline) for 10,000 generations, collecting and
572 freezing samples at -80 °C every 70 generations. The remaining wells contained blank controls or
573 populations of other yeast species and will be described elsewhere. This is the same procedure
574 used to generate the compared *S. cerevisiae* dataset[3]. Because these conditions yield a doubling
575 rate of 10 generations per day, we performed a 1/1024 serial dilution every day ($1/2^{10}$). This
576 corresponds to an effective population size of ~6.00E04 and a bottleneck population size of
577 ~8.00E03 [3,115]. We chose to perform whole-population whole-genome sequencing every 1,000
578 generations, and we were able to grow back cells from 93 out of these 100 samples after storage
579 and sequenced these time points with Illumina NovaSeq paired-end sequencing (mean effective
580 coverage ~40X). Raw DNA sequences are available on NCBI:
581 https://www.ncbi.nlm.nih.gov/bioproject/PRJNA1315931.

582

583 **Measuring fitness in the *S. pombe* populations**

584 We grew the evolved populations, the WT, and a *S. cerevisiae* reference strain expressing GFP
585 (YAN438: *MAT*α *his3*Δ1 *ura3*Δ0 *leu2*Δ0 *lys2*Δ0 *can1*::*RPL39pr-ymGFP_STE2pr-*

586 *SpHIS5_STE3pr-LEU2*), for 24 hours. In contrast to our previous study[3], this *S. cerevisiae* strain
587 does not express a killer phenotype as it does not possess ScV-M1 killer-virus RNA. Next, because
588 the green *S. cerevisiae* strain grew much faster than *S. pombe,* we prepared mixtures of the "dark"
589 *S. pombe* populations and the green budding yeast at a 9:1 ratio and grew the mixed cultures for
590 24 hours. This ratio also reduces potential species interactions between *S. cerevisiae* and *S. pombe*.
591 We then serially propagated each mixture for 3 days and used a Beckman-Coulter CytoFlex flow
592 cytometer to measure the frequency of the "dark" *S. pombe* and the green *S. cerevisiae* strain daily.
593 All particle counts were acquired at 30 µL/s rate for a maximum of 60 seconds or until 10,000
594 events were detected from a 96-well plate containing the mixtures. The data were analyzed using
595 the CytoFlex acquisition and analysis software CytExpert. The "dark" *S. pombe* cells were
596 distinguished from the green *S. cerevisiae* strain using FITC-A/PE-A gates. This process was
597 replicated on a different day for biological replicates. Using the cell counts, we then calculated the
598 frequency of each population in the mixture and inferred fitness based on the slope of a linear
599 regression between the logarithm of the frequency ratio and the number of generations:

600 $$\ln\left(\frac{frequency_{S.\ pombe}}{frequency_{green\ S.\ cerevisiae}}\right) = (Fitness * number\ of\ generations) + intercept \qquad \text{(Eq. 1)}$$

601

602 The final fitness was the average of the two biological replicates.

603 **Variant calling**

604 We used Varscan2.4.6[47] to call single-nucleotide variants (SNVs) and indels. Because
605 contamination, sequencing errors and low-complexity regions can affect the variant calling, we
606 applied some filters to the called variants (Table 2). These filters ensure that the calls are supported
607 by reads, are time-consistent, and are not affected by possible errors in the reference genome, e.g.
608 avoiding confusion between ancestral alleles that were not present in the reference genome (972h-
609 ) and fixed de novo mutations. Briefly, the filters used mapping and read base quality, allele
610 frequency and absence of strand biases. In addition, because of the relatively sparse sequencing of
611 our experiment (every 1000 generations), most genuine mutations will be fixed in cohorts or
612 throughout the experiment, we also employed a filter for genetic hitchhiking and clonality. The
613 variant calling pipeline is available at
614 https://github.com/arnaud00013/Experimental_evolution_S_pombe.

| Filter name | Criteria |
|---|---|
| Mapping quality | Mapping quality score ≥ 15 |
| Indels in low-complexity regions (short tandem repeats or homopolymers) | -Systematically eliminate the ones that are not supported by multiple samples<br>-For the recurrent ones, because they could reveal a signal of selection, they were manually investigated in IGV to make sure there are no mapping mistakes, and multiple reads in both strands should support them. We also ensured that they were not introduced or fixed at the same time across multiple |

| | |
|---|---|
| | populations or systematically with the same group of alleles (**Fig. 3**), which could indicate contamination. |
| Read bases quality | ≥ Q20 |
| Allele frequency | ≥ 0.05 |
| Coverage and supporting reads | Coverage ≥ 5 and at least one read in both strands support the variant (so at least 2 supporting reads in total, and always 2 supporting strands) |
| Contamination | Because the *S. pombe* populations were grown in parallel with populations from other yeast species (*C. glabrata* CBS138, *K. lactis* NRRL-Y-1140, *P. pastoris* EAMORG09, *S. cerevisiae* YJM978, *S. paradoxus* IFO1804; **Fig. 1**), we made sure that the reads we recovered from sequencing best map to *S. pombe* |
| Evidence for sub-clonality and linkage disequilibrium | \|Pearson r\| ≥ 0.9 with at least one mutation from the same population |
| Variation in non-fixed variant allele frequency | ≥ 0.1 |
| Initial allele frequency | Eliminate variants with an allele frequency ≥ 0.4 in at least a third of the populations |

**Table 2** List of variant calling filters.

**Identifying signatures of selection from the substitution spectrum**

We defined substitutions as variants with an allele frequency >= 75%. Then, we compared the substitution spectrum of each population with the one expected after 10,000 generations of evolution under a neutral null model. The number of fixed variants in each mutation category is calculated based on the species' evolution rate, genome size, genome architecture (e.g. ratio of coding to non-coding regions in the genome), and the proportion of single-nucleotide mutations derived from the genetic code and associated with a specific category of mutations. This allowed to derive 2 equations:

$$Nb_subs_in_category_X_nm = S_{rate} * t * G_{size} * r_x * p_x \quad \text{(Eq. 2)}$$

$$Nb_indels_in_category_X_nm = I_{rate} * t * G_{size} * r_x \quad \text{(Eq. 3)}$$

where $Nb_subs_in_category_X_nm$ is the expected number of substitutions in a mutation category X assuming a neutral model of evolution, $Nb_indels_in_category_X_nm$ is the expected number of indels of type X assuming a neutral model of evolution, $S_{rate}$ is the species substitution rate, $I_{rate}$ is the species indel rate, t is the number of generations observed since the start of the experiment, $G_{size}$ is the species genome size, $r_x$ is the proportion of the genome covered by protein-coding or non-coding sites, depending on the mutation category X and $p_x$ is the

633 proportion of single-nucleotide mutations derived from the genetic code that can be classified as
634 mutations from category X.

635 Next, we sought signatures of parallelism and positive selection in protein-coding genes
636 among the fixed variants. We defined a "hit" as a fixed variant that is not synonymous (missense,
637 nonsense, or indel), and a multi-hit gene as a gene with hits in multiple populations. (in at least 2
638 out of 10 populations). We then compared the number of population hits (PH) in the set of multi-
639 hit genes to the PH expected under a null model, assuming that all genes evolve and fix variants
640 at the same rate. The expected PH was determined based on a number drawn from a Poisson
641 distribution where the argument λ (average number of events per interval) is the product of S.
642 pombe's substitution rate, the gene length, the generation time, the number of populations, and the
643 proportion of fixed variants that are not synonymous as determined in equations 2 and 3.

644 **Evaluating and comparing the sensitivity to hydrogen peroxide**

645 We grew the 10 evolved *S. pombe* populations and the WT ancestor in the rows of a 96-well plate
646 at 30°C for 36 hours. The media was YPD + hydrogen peroxide with $H_2O_2$ concentrations of 0
647 mM, 0.5 mM, 1 mM, 1.5 mM, 2 mM, 2.5 mM, 3 mM and 3.5 mM. Each row of the 96-well plate
648 corresponded to a different concentration of $H_2O_2$. The growth of each population was estimated
649 using the OD600 time series measured from a BioTek Synergy HTX plate reader. For each time
650 series, the area under the curve (AUC) was measured using the R package package
651 growthcurver[116]. Using the AUC as a proxy for growth, we then compared the AUC of each
652 population at different $H_2O_2$ concentrations to the AUC obtained when $H_2O_2$ is absent from the
653 media. Next, we inferred the degree of inhibition with:

654 $$Inhibition = k * \frac{AUC_{media}}{AUC_{control}} \quad \text{(Eq. 4)}$$

655 where $k$ is a normalizing factor that makes sure the inhibition metric maximum is 1, AUC is the
656 area under the growth curve, $AUC_{media}$ represents the growth at a certain concentration of
657 hydrogen peroxide and $AUC_{control}$ represents the growth in a YPD media without hydrogen
658 peroxide. This expression is negatively correlated to the AUC ratio and ranges from 0 to 1. Using
659 the Dose-Response Analysis R package drc[117], we then fitted a log-logistic model to this metric
660 and $H_2O_2$ concentrations to estimate the IC50, which recapitulates the level of sensitivity of a
661 population to hydrogen peroxide. Data in the manuscript is a representative result of the less noisy
662 biological replicate. We found that the hydrogen peroxide concentration tended to vary due to
663 instability of the chemical, which would at times shift the IC50, without changing the interpretation
664 of the experiment. Finally, we performed a cluster analysis on the populations based on their
665 distribution of AUC media-to-control ratio at different concentrations. We used the hclust function
666 from the package stats v4.1.2[118] to perform the clustering and the composition of each cluster was
667 identical no matter the distance metric tested (Gower, Manhattan, Euclidean, Bray-Curtis), which
668 we obtained with the function vegdist from the package vegan 2.7-2[119].

669 **RNA extraction, sequencing and transcriptomic analysis**

670 We extracted in two biological replicates the RNA of the evolved populations using an in-house
671 protocol that works well with *S. cerevisiae*. Briefly, cells were grown to mid-log phase in YPD by

672 diluted overnight saturated cultures and growing for 4-6 hours and lysed using 100 µl of 5 mg/mL
673 Zymolyase + 10 mM DTT, incubated at 37 °Celsius for 5 minutes. The weakened cells were then
674 incubated with 100 µl of 2% SDS for a final SDS concentration of 1%. 200 µl of lysis buffer was
675 added (4.5 M Guanidine thiocyanate, 10 mM EDTA) and mixed gently by inverting. Lysate
676 clarification indicated complete lysis. The SDS was then precipitated using 200 µl of 3M
677 Potassium acetate at pH 5.

678 After centrifugation, the lysate was passed through a minipreparation silica column to bind DNA.
679 Under these conditions, RNA does not bind to the silica columns. Therefore, we collected the
680 flowthrough. We then mixed it with an equal volume of pure isopropanol and passed it through
681 another minipreparation silica column (which will now bind RNA). The column was then washed
682 with 400 µl of wash buffer (10% Guanidine thiocyanate, 25% Isopropanol, and 10 mM EDTA),
683 and then twice with 600 µl of 80% Ethanol. After drying the column, the RNA was eluted with 50
684 µl of 10 mM Tris pH 8.5. RNA integrity was verified on an agarose gel. One population (H12)
685 failed to get sufficiently high-quality RNA for sequencing.

686 We sequenced the successfully extracted RNA using NEBNext Ultra II on an Illumina NovaSeq
687 X paired-end sequencing lane. This yielded 10.6E06 150-bp paired-end reads per sample on
688 average (σ=1.32E06). Raw RNA-sequencing data are available on NCBI:
689 https://www.ncbi.nlm.nih.gov/bioproject/PRJNA1315931. We pre-processed the reads with fastp
690 (version 0.23.1) with the arguments --trim_poly_x --trim_poly_g --cut_front --
691 cut_front_mean_quality 20 --cut_tail --cut_tail_mean_quality 20 --detect_adapter_for_pe[120].
692 Next, we mapped the reads to the reference (972h-) using samtools v1.17, removed duplicates with
693 picard v2.26.3 and counted the number of reads per gene using featureCounts from subread
694 v2.0.6[121–123], and the counts were converted to FPKM. We then performed PCA analysis of the
695 transcriptome and found two main clusters (PC1 and PC2 explained about 75% of the
696 transcriptomic variance), one which contained the WT and the other contained only populations
697 that were more sensitive to oxidative stress than WT. One population that was as sensitive as WT
698 clustered independently, and two populations that clustered with the WT were more sensitive to
699 oxidative stress. Upon analysis of their gene hits, we found that they have loss-of-function
700 mutation in genes that relate to oxidative stress resistance.

701 To determine which genes and their expression differences were responsible for the increased
702 oxidative stress sensitivity of most populations, we used the DESeq2 package to detect
703 differentially expressed genes between the two clusters (i.e. populations that are as sensitive and
704 more sensitive than WT)[124]. The RNA-seq analysis pipeline is available at
705 https://github.com/arnaud00013/Experimental_evolution_S_pombe.

706 **REFERENCES**


707 1. Kryazhimskiy, S., Rice, D. P., Jerison, E. R. & Desai, M. M. Microbial evolution. Global epistasis
708 makes adaptation predictable despite sequence-level stochasticity. *Science* **344**, 1519–1522
709 (2014).
710 2. Couce, A. & Tenaillon, O. A. The rule of declining adaptability in microbial evolution
711 experiments. *Front Genet* **6**, 99 (2015).
712 3. Johnson, M. S. *et al.* Phenotypic and molecular evolution across 10,000 generations in
713 laboratory budding yeast populations. *eLife* **10**, e63910 (2021).
714 4. Good, B. H., McDonald, M. J., Barrick, J. E., Lenski, R. E. & Desai, M. M. The dynamics of
715 molecular evolution over 60,000 generations. *Nature* **551**, 45–50 (2017).
716 5. Kinnersley, M. *et al.* Ex Uno Plures: Clonal Reinforcement Drives Evolution of a Simple
717 Microbial Community. *PLOS Genetics* **10**, e1004430 (2014).
718 6. Tenaillon, O. *et al.* Tempo and mode of genome evolution in a 50,000-generation experiment.
719 *Nature* **536**, 165–170 (2016).
720 7. Lang, G. I. *et al.* Pervasive genetic hitchhiking and clonal interference in forty evolving yeast
721 populations. *Nature* **500**, 571–574 (2013).
722 8. Venkataram, S. *et al.* Development of a Comprehensive Genotype-to-Fitness Map of
723 Adaptation-Driving Mutations in Yeast. *Cell* **166**, 1585-1596.e22 (2016).
724 9. Jerison, E. R. *et al.* Genetic variation in adaptability and pleiotropy in budding yeast. *eLife* **6**,
725 e27167.
726 10. Burke, M. K. *et al.* Genome-wide analysis of a long-term evolution experiment with Drosophila.
727 *Nature* **467**, 587–590 (2010).
728 11. Stroud, J. T. & Ratcliff, W. C. Long-term studies provide unique insights into evolution. *Nature*
729 **639**, 589–601 (2025).

730 12. Bakerlee, C. W., Ba, A. N. N., Shulgina, Y., Echenique, J. I. R. & Desai, M. M. Idiosyncratic
731 epistasis leads to global fitness-correlated trends. *Science* **376**, 630–635 (2022).
732 13. Echenique, J. I. R., Kryazhimskiy, S., Ba, A. N. N. & Desai, M. M. Modular epistasis and the
733 compensatory evolution of gene deletion mutants. *PLOS Genetics* **15**, e1007958 (2019).
734 14. Helsen, J. *et al.* Gene Loss Predictably Drives Evolutionary Adaptation. *Molecular Biology and*
735 *Evolution* **37**, 2989–3002 (2020).
736 15. Teng, X. *et al.* Genome-wide consequences of deleting any single gene. *Mol Cell* **52**, 485–494
737 (2013).
738 16. Galardini, M. *et al.* The impact of the genetic background on gene deletion phenotypes in
739 Saccharomyces cerevisiae. *Mol Syst Biol* **15**, e8831 (2019).
740 17. Blount, Z. D., Borland, C. Z. & Lenski, R. E. Historical contingency and the evolution of a key
741 innovation in an experimental population of Escherichia coli. *Proc Natl Acad Sci U S A* **105**,
742 7899–7906 (2008).
743 18. Huang, M.-E., Rio, A.-G., Nicolas, A. & Kolodner, R. D. A genomewide screen in Saccharomyces
744 cerevisiae for genes that suppress the accumulation of mutations. *Proceedings of the National*
745 *Academy of Sciences* **100**, 11529–11534 (2003).
746 19. Opulente, D. A. *et al.* Genomic factors shape carbon and nitrogen metabolic niche breadth
747 across Saccharomycotina yeasts. *Science* **384**, eadj4503 (2024).
748 20. Shen, X.-X. *et al.* Tempo and Mode of Genome Evolution in the Budding Yeast Subphylum. *Cell*
749 **175**, 1533-1545.e20 (2018).
750 21. Frost, A. *et al.* Comparing S. pombe and S. cerevisiae Genetic Interactions Reveals Functional
751 Repurposing and Identifies New Organelle Homeostasis and Mitosis Control Genes. *Cell* **149**,
752 1339–1352 (2012).

753 22. Rhind, N. *et al.* Comparative Functional Genomics of the Fission Yeasts. *Science* **332**, 930–936
754 (2011).
755 23. Forsburg, S. L. Overview of. *Current Protocols in Molecular Biology* **64**, 13.14.1-13.14.3 (2003).
756 24. Vyas, A., Freitas, A. V., Ralston, Z. A. & Tang, Z. Fission Yeast Schizosaccharomyces pombe: A
757 Unicellular "Micromammal" Model Organism. *Curr Protoc* **1**, e151 (2021).
758 25. Ward, C. M. *et al.* Recombination, admixture and genome instability shape the genomic
759 landscape of Saccharomyces cerevisiae derived from spontaneous grape ferments. *PLoS*
760 *Genet* **20**, e1011223 (2024).
761 26. Peter, J. *et al.* Genome evolution across 1,011 Saccharomyces cerevisiae isolates. *Nature* **556**,
762 339–344 (2018).
763 27. Chen, V. *et al.* Evolution of haploid and diploid populations reveals common, strong, and
764 variable pleiotropic effects in non-home environments. *eLife* **12**, e92899 (2023).
765 28. Shapira, R., Levy, T., Shaked, S., Fridman, E. & David, L. Extensive heterosis in growth of yeast
766 hybrids is explained by a combination of genetic models. *Heredity (Edinb)* **113**, 316–326 (2014).
767 29. Shapira, R. & David, L. Genes with a Combination of Over-Dominant and Epistatic Effects
768 Underlie Heterosis in Growth of Saccharomyces cerevisiae at High Temperature. *Front Genet*
769 **7**, 72 (2016).
770 30. Conant, G. C. & Wolfe, K. H. Increased glycolytic flux as an outcome of whole-genome
771 duplication in yeast. *Mol Syst Biol* **3**, 129 (2007).
772 31. Vowinckel, J. *et al.* The metabolic growth limitations of petite cells lacking the mitochondrial
773 genome. *Nat Metab* **3**, 1521–1535 (2021).
774 32. Alam, S., Gu, Y., Reichert, P., Bähler, J. & Oliferenko, S. Optimization of energy production and
775 central carbon metabolism in a non-respiring eukaryote. *Current Biology* **33**, 2175-2186.e5
776 (2023).

33. Chen, X. J. & Clark-Walker, G. D. The petite mutation in yeasts: 50 years on. *Int Rev Cytol* **194**, 197–238 (2000).
34. Dashko, S., Zhou, N., Compagno, C. & Piškur, J. Why, when, and how did yeast evolve alcoholic fermentation? *FEMS Yeast Res* **14**, 826–832 (2014).
35. Kamrad, S. *et al.* Pyruvate kinase variant of fission yeast tunes carbon metabolism, cell regulation, growth and stress resistance. *Mol Syst Biol* **16**, e9270 (2020).
36. Bergström, A. *et al.* A High-Definition View of Functional Genetic Variation from Natural Yeast Genomes. *Molecular Biology and Evolution* **31**, 872–888 (2014).
37. Farlow, A. *et al.* The Spontaneous Mutation Rate in the Fission Yeast Schizosaccharomyces pombe. *Genetics* **201**, 737–744 (2015).
38. Wood, V. *et al.* The genome sequence of Schizosaccharomyces pombe. *Nature* **415**, 871–880 (2002).
39. Blevins, W. R. *et al.* Uncovering de novo gene birth in yeast using deep transcriptomics. *Nat Commun* **12**, 604 (2021).
40. Harris, M. A. *et al.* Fission stories: using PomBase to understand Schizosaccharomyces pombe biology. *Genetics* **220**, iyab222 (2022).
41. Behringer, M. G. & Hall, D. W. Genome-Wide Estimates of Mutation Rates and Spectrum in Schizosaccharomyces pombe Indicate CpG Sites are Highly Mutagenic Despite the Absence of DNA Methylation. *G3 (Bethesda)* **6**, 149–160 (2015).
42. Schlackow, M. & Gullerova, M. Understanding non-coding DNA regions in yeast. *Biochemical Society Transactions* **41**, 1654–1659 (2013).
43. Ohsawa, S. *et al.* Nitrogen signaling factor triggers a respiration-like gene expression program in fission yeast. *The EMBO Journal* **43**, 4604–4624 (2024).

800 44. Vassiliadis, D., Wong, K. H., Andrianopoulos, A. & Monahan, B. J. A genome-wide analysis of
801 carbon catabolite repression in Schizosaccharomyces pombe. *BMC Genomics* **20**, 251 (2019).
802 45. Landolfo, S., Politi, H., Angelozzi, D. & Mannazzu, I. ROS accumulation and oxidative damage
803 to cell structures in *Saccharomyces cerevisiae* wine strains during fermentation of high-sugar-
804 containing medium. *Biochimica et Biophysica Acta (BBA) - General Subjects* **1780**, 892–898
805 (2008).
806 46. Synnott, J. M., Guida, A., Mulhern-Haughey, S., Higgins, D. G. & Butler, G. Regulation of the
807 Hypoxic Response in Candida albicans. *Eukaryot Cell* **9**, 1734–1746 (2010).
808 47. Koboldt, D. C. *et al.* VarScan 2: somatic mutation and copy number alteration discovery in
809 cancer by exome sequencing. *Genome Res* **22**, 568–76 (2012).
810 48. Koboldt, D. C. Best practices for variant calling in clinical sequencing. *Genome Medicine* **12**, 91
811 (2020).
812 49. Li, H. Toward better understanding of artifacts in variant calling from high-coverage samples.
813 *Bioinformatics* **30**, 2843–2851 (2014).
814 50. Zhu, Y. O., Siegal, M. L., Hall, D. W. & Petrov, D. A. Precise estimates of mutation rate and
815 spectrum in yeast. *Proceedings of the National Academy of Sciences of the United States of*
816 *America* **111**, E2310 (2014).
817 51. Lynch, M. *et al.* A genome-wide view of the spectrum of spontaneous mutations in yeast.
818 *Proceedings of the National Academy of Sciences of the United States of America* **105**, 9272
819 (2008).
820 52. Schacherer, J., Shapiro, J. A., Ruderfer, D. M. & Kruglyak, L. Comprehensive polymorphism
821 survey elucidates population structure of S. cerevisiae. *Nature* **458**, 342–345 (2009).
822 53. Gallone, B. *et al.* Origins, evolution, domestication and diversity of *Saccharomyces* beer
823 yeasts. *Current Opinion in Biotechnology* **49**, 148–155 (2018).

824 54. Duan, S.-F. *et al.* The origin and adaptive evolution of domesticated populations of yeast from
825 Far East Asia. *Nat Commun* **9**, 2690 (2018).
826 55. Chen, H., Blum, J. E., Thalacker-Mercer, A. & Gu, Z. Impact of the Whole Genome Duplication
827 Event on PYK Activity and Effects of a PYK1 Mutation on Metabolism in S. cerevisiae. *Front Mol*
828 *Biosci* **8**, 656461 (2021).
829 56. Frost, A. *et al.* Comparing S. pombe and S. cerevisiae Genetic Interactions Reveals Functional
830 Repurposing and Identifies New Organelle Homeostasis and Mitosis Control Genes. *Cell* **149**,
831 1339 (2012).
832 57. Aslett, M. & Wood, V. Gene Ontology annotation status of the fission yeast genome: preliminary
833 coverage approaches 100%. *Yeast* **23**, 913–919 (2006).
834 58. Khan, T., Douglas, G. M., Patel, P., Nguyen Ba, A. N. & Moses, A. M. Polymorphism Analysis
835 Reveals Reduced Negative Selection and Elevated Rate of Insertions and Deletions in
836 Intrinsically Disordered Protein Regions. *Genome Biology and Evolution* **7**, 1815–1826 (2015).
837 59. Dean, E. J., Davis, J. C., Davis, R. W. & Petrov, D. A. Pervasive and Persistent Redundancy
838 among Duplicated Genes in Yeast. *PLOS Genetics* **4**, e1000113 (2008).
839 60. Kim, D.-U. *et al.* Analysis of a genome-wide set of gene deletions in the fission yeast
840 Schizosaccharomyces pombe. *Nat Biotechnol* **28**, 617–623 (2010).
841 61. Dupré, S., Urban-Grimal, D. & Haguenauer-Tsapis, R. Ubiquitin and endocytic internalization in
842 yeast and animal cells. *Biochimica et Biophysica Acta (BBA) - Molecular Cell Research* **1695**,
843 89–111 (2004).
844 62. Zattas, D. & Hochstrasser, M. Ubiquitin-dependent Protein Degradation at the Yeast
845 Endoplasmic Reticulum and Nuclear Envelope. *Crit Rev Biochem Mol Biol* **50**, 1–17 (2015).
846 63. Lee, C.-Y. S., Yeh, T.-L., Hughes, B. T. & Espenshade, P. J. Regulation of the Sre1 hypoxic
847 transcription factor by oxygen-dependent control of DNA binding. *Mol Cell* **44**, 225–234 (2011).

848 64. Hughes, B. T. & Espenshade, P. J. Oxygen-regulated degradation of fission yeast SREBP by
849 Ofd1, a prolyl hydroxylase family member. *EMBO J* **27**, 1491–1501 (2008).
850 65. Porter, J. R., Lee, C.-Y. S., Espenshade, P. J. & Iglesias, P. A. Regulation of SREBP during hypoxia
851 requires Ofd1-mediated control of both DNA bindingand degradation. *Mol Biol Cell* **23**, 3764–
852 3774 (2012).
853 66. Matsuda, S., Kikkawa, U., Uda, H. & Nakashima, A. The S. pombe CDK5 ortholog Pef1 regulates
854 sexual differentiation through control of the TORC1 pathway and autophagy. *Journal of Cell*
855 *Science* **133**, jcs247817 (2020).
856 67. Todd, B. L., Stewart, E. V., Burg, J. S., Hughes, A. L. & Espenshade, P. J. Sterol Regulatory
857 Element Binding Protein Is a Principal Regulator of Anaerobic Gene Expression in Fission Yeast.
858 *Mol Cell Biol* **26**, 2817–2831 (2006).
859 68. Farrugia, G. & Balzan, R. Oxidative Stress and Programmed Cell Death in Yeast. *Front. Oncol.* **2**,
860 (2012).
861 69. Kaino, T., Tonoko, K., Mochizuki, S., Takashima, Y. & Kawamukai, M. Schizosaccharomyces
862 japonicus has low levels of CoQ10 synthesis, respiration deficiency, and efficient ethanol
863 production. *Bioscience, Biotechnology, and Biochemistry* **82**, 1031–1042 (2018).
864 70. Rodríguez-López, M. *et al.* Broad functional profiling of fission yeast proteins using phenomics
865 and machine learning. *eLife* **12**, RP88229 (2023).
866 71. Philpott, C. C., Leidgens, S. & Frey, A. G. Metabolic remodeling in iron-deficient fungi.
867 *Biochimica et Biophysica Acta (BBA) - Molecular Cell Research* **1823**, 1509–1520 (2012).
868 72. Rubio, A., Ghosh, S., Mülleder, M., Ralser, M. & Mata, J. Ribosome profiling reveals ribosome
869 stalling on tryptophan codons and ribosome queuing upon oxidative stress in fission yeast.
870 *Nucleic Acids Research* **49**, 383–399 (2021).

871 73. Kwon, E.-J. G. *et al.* Deciphering the Transcriptional-Regulatory Network of Flocculation in
872 Schizosaccharomyces pombe. *PLoS Genet* **8**, e1003104 (2012).
873 74. Stewart, G. G. Yeast Flocculation—Sedimentation and Flotation. *Fermentation* **4**, 28 (2018).
874 75. Dyson, H. J. & Wright, P. E. Intrinsically unstructured proteins and their functions. *Nat Rev Mol*
875 *Cell Biol* **6**, 197–208 (2005).
876 76. Chen, D. *et al.* Global Transcriptional Responses of Fission Yeast to Environmental Stress. *Mol*
877 *Biol Cell* **14**, 214–229 (2003).
878 77. Sawada, N., Ueno, S. & Takeda, K. Regulation of inorganic polyphosphate is required for proper
879 vacuolar proteolysis in fission yeast. *J Biol Chem* **297**, 100891 (2021).
880 78. Calvo, I. A., García, P., Ayté, J. & Hidalgo, E. The transcription factors Pap1 and Prr1 collaborate
881 to activate antioxidant, but not drug tolerance, genes in response to H2O2. *Nucleic Acids Res*
882 **40**, 4816–4824 (2012).
883 79. Quinn, J. *et al.* Two-Component Mediated Peroxide Sensing and Signal Transduction in Fission
884 Yeast. *Antioxidants & Redox Signaling* **15**, 153–165 (2011).
885 80. Leiter, É. *et al.* Protein phosphatase Z modulates oxidative stress response in fungi. *Fungal*
886 *Genet Biol* **49**, 708–716 (2012).
887 81. Matsuo, Y. *et al.* Polypeptone Induces Dramatic Cell Lysis in ura4 Deletion Mutants of Fission
888 Yeast. *PLOS ONE* **8**, e59887 (2013).
889 82. Kosugi, M. *et al.* Stereochemical assignment of the unique electron acceptor 5'-
890 hydroxyphylloquinone, a polar analog of vitamin K1 in photosystem I. *Biosci Biotechnol*
891 *Biochem* **81**, 2244–2252 (2017).
892 83. Hughes, A. L., Todd, B. L. & Espenshade, P. J. SREBP pathway responds to sterols and
893 functions as an oxygen sensor in fission yeast. *Cell* **120**, 831–842 (2005).

894 84. Miki, R., Saiki, R., Ozoe, Y. & Kawamukai, M. Comparison of a coq7 deletion mutant with other
895 respiration-defective mutants in fission yeast. *The FEBS Journal* **275**, 5309–5324 (2008).
896 85. Pluskal, T., Sajiki, K., Becker, J., Takeda, K. & Yanagida, M. Diverse fission yeast genes required
897 for responding to oxidative and metal stress: Comparative analysis of glutathione-related and
898 other defense gene deletions. *Genes to Cells* **21**, 530–542 (2016).
899 86. Uchida, N. *et al.* Phenotypes of Fission Yeast Defective in Ubiquinone Production Due to
900 Disruption of the Gene for p-Hydroxybenzoate Polyprenyl Diphosphate Transferase. *J Bacteriol*
901 **182**, 6933–6939 (2000).
902 87. Wittkopp, P. J., Haerum, B. K. & Clark, A. G. Evolutionary changes in cis and trans gene
903 regulation. *Nature* **430**, 85–88 (2004).
904 88. Wittkopp, P. J. & Kalay, G. Cis-regulatory elements: molecular mechanisms and evolutionary
905 processes underlying divergence. *Nat Rev Genet* **13**, 59–69 (2011).
906 89. Liu, X., Li, Y. I. & Pritchard, J. K. Trans Effects on Gene Expression Can Drive Omnigenic
907 Inheritance. *Cell* **177**, 1022-1034.e6 (2019).
908 90. Yao, C. *et al.* Dynamic Role of trans Regulation of Gene Expression in Relation to Complex
909 Traits. *Am J Hum Genet* **100**, 571–580 (2017).
910 91. Renganaath, K. & Albert, F. W. Trans-eQTL hotspots shape complex traits by modulating
911 cellular states. *bioRxiv* 2023.11.14.567054 (2024) doi:10.1101/2023.11.14.567054.
912 92. Zakrzewska, A. *et al.* Genome-wide analysis of yeast stress survival and tolerance acquisition
913 to analyze the central trade-off between growth rate and cellular robustness. *Mol Biol Cell* **22**,
914 4435–4446 (2011).
915 93. Alejandro-Osorio, A. L. *et al.* The histone deacetylase Rpd3p is required for transient changes
916 in genomic expression in response to stress. *Genome Biol* **10**, R57 (2009).

917 94. Balcells, L. *et al*. The Pzh1 protein phosphatase and the Spm1 protein kinase are involved in the
918 regulation of the plasma membrane H+-ATPase in fission yeast. *FEBS Letters* **435**, 241–244
919 (1998).
920 95. Shahrouzi, P., Forouz, F., Mathelier, A., Kristensen, V. N. & Duijf, P. H. G. Copy number
921 alterations: a catastrophic orchestration of the breast cancer genome. *Trends in Molecular*
922 *Medicine* **30**, 750–764 (2024).
923 96. Al Tameemi, W., Dale, T. P., Al-Jumaily, R. M. K. & Forsyth, N. R. Hypoxia-Modified Cancer Cell
924 Metabolism. *Front. Cell Dev. Biol.* **7**, (2019).
925 97. Steele, C. D. *et al*. Signatures of copy number alterations in human cancer. *Nature* **606**, 984–
926 991 (2022).
927 98. Denver, D. R., Morris, K., Lynch, M. & Thomas, W. K. High mutation rate and predominance of
928 insertions in the Caenorhabditis elegans nuclear genome. *Nature* **430**, 679–682 (2004).
929 99. Jensen, L. T. & Culotta, V. C. Regulation of *Saccharomyces cerevisiae FET4* by Oxygen and Iron.
930 *Journal of Molecular Biology* **318**, 251–260 (2002).
931 100. Daskalaki, I., Gkikas, I. & Tavernarakis, N. Hypoxia and Selective Autophagy in Cancer
932 Development and Therapy. *Front Cell Dev Biol* **6**, 104 (2018).
933 101. Slomka, S. *et al*. Experimental Evolution of Bacillus subtilis Reveals the Evolutionary
934 Dynamics of Horizontal Gene Transfer and Suggests Adaptive and Neutral Effects. *Genetics*
935 **216**, 543–558 (2020).
936 102. McDonald, M. J. Microbial Experimental Evolution - a proving ground for evolutionary theory
937 and a tool for discovery. *EMBO Rep* **20**, e46992 (2019).
938 103. Chaudhuri, B., Ingavale, S. & Bachhawat, A. K. Apd1(+), a Gene Required for Red Pigment
939 Formation in Ade6 Mutants of Schizosaccharomyces Pombe, Encodes an Enzyme Required for

940 Glutathione Biosynthesis: A Role for Glutathione and a Glutathione-Conjugate Pump. *Genetics*
941 **145**, 75–83 (1997).
942 104. Li, Y. *et al.* Hidden Complexity of Yeast Adaptation under Simple Evolutionary Conditions.
943 *Current Biology* **28**, 515-525.e6 (2018).
944 105. Williamson, T., Adiamah, D., Schwartz, J.-M. & Stateva, L. Exploring the genetic control of
945 glycolytic oscillations in Saccharomyces Cerevisiae. *BMC Systems Biology* **6**, 108 (2012).
946 106. Cytryńska, M., Frajnt, M. & Jakubowicz, T. Saccharomyces cerevisiae pyruvate kinase Pyk1
947 is PKA phosphorylation substrate in vitro. *FEMS Microbiology Letters* **203**, 223–227 (2001).
948 107. Yu, Z.-Q. *et al.* Atg38-Atg8 interaction in fission yeast establishes a positive feedback loop
949 to promote autophagy. *Autophagy* **16**, 2036–2051 (2020).
950 108. Zhao, D. *et al.* Atg20- and Atg24-family proteins promote organelle autophagy in fission
951 yeast. *J Cell Sci* **129**, 4289–4304 (2016).
952 109. Su, Y., Chen, C., Huang, L., Yan, J. & Huang, Y. Schizosaccharomyces pombe Homologs of
953 Human DJ-1 Are Stationary Phase-Associated Proteins That Are Involved in Autophagy and
954 Oxidative Stress Resistance. *PLOS ONE* **10**, e0143888 (2015).
955 110. Blanco, M. *et al.* An approach to the hypoxic and oxidative stress responses in
956 Kluyveromyces lactis by analysis of mRNA levels. *FEMS Yeast Research* **7**, 702–714 (2007).
957 111. Liu, J. & Barrientos, A. Transcriptional Regulation of Yeast Oxidative Phosphorylation
958 Hypoxic Genes by Oxidative Stress. *Antioxidants & Redox Signaling* **19**, 1916–1927 (2013).
959 112. Liu, J. & Wang, Z. Increased Oxidative Stress as a Selective Anticancer Therapy. *Oxid Med*
960 *Cell Longev* **2015**, 294303 (2015).
961 113. Mendoza, E. N., Ciriolo, M. R. & Ciccarone, F. Hypoxia-Induced Reactive Oxygen Species:
962 Their Role in Cancer Resistance and Emerging Therapies to Overcome It. *Antioxidants* **14**, 94
963 (2025).

964 114. She, H. *et al.* Gene expression plasticity followed by genetic change during colonization a
965 high-elevation environment. *eLife* **12**, (2023).
966 115. Wahl, L. M. & Gerrish, P. J. The probability that beneficial mutations are lost in populations
967 with periodic bottlenecks. *Evolution* **55**, 2606–2610 (2001).
968 116. Sprouffske, K. & Wagner, A. Growthcurver: an R package for obtaining interpretable metrics
969 from microbial growth curves. *BMC Bioinformatics* **17**, 172 (2016).
970 117. Ritz, C., Baty, F., Streibig, J. C. & Gerhard, D. Dose-Response Analysis Using R. *PLOS ONE*
971 **10**, e0146021 (2015).
972 118. R Core Team. *R: A Language and Environment for Statistical Computing*. (R Foundation for
973 Statistical Computing, Vienna, Austria, 2021).
974 119. Oksanen, J. *et al. Vegan: Community Ecology Package*. (2025).
975 120. Chen, S., Zhou, Y., Chen, Y. & Gu, J. fastp: an ultra-fast all-in-one FASTQ preprocessor.
976 *Bioinformatics* **34**, i884–i890 (2018).
977 121. Li, H. *et al.* The Sequence Alignment/Map format and SAMtools. *Bioinformatics* **25**, 2078–
978 2079 (2009).
979 122. Picard toolkit. *Broad Institute, GitHub repository* (2019).
980 123. Liao, Y., Smyth, G. K. & Shi, W. featureCounts: an efficient general purpose program for
981 assigning sequence reads to genomic features. *Bioinformatics* **30**, 923–930 (2014).
982 124. Love, M. I., Huber, W. & Anders, S. Moderated estimation of fold change and dispersion for
983 RNA-seq data with DESeq2. *Genome Biol* **15**, 550 (2014).
984